Gas and Energy Transition Research Centre

31 October 2025

The University Of Queensland
AUSTRALIA
CREATE CHANGE

Long-term back-casting of wind & solar capacity factors for the ISP Renewable Energy Zones

Project

This report was produced through an independent research investigation by the UQ Gas & Energy Transition Research Centre (UQ-GET). It responds to a growing recognition by energy system stakeholders that improved uncertainty analysis will be critical to enabling an effective energy transition.

Research Team

Dr Joe Lane, Senior Research Fellow, UQ Gas and Energy Transition Research Centre

Dr Nathan Di Vaira, Research Fellow, UQ Gas and Energy Transition Research Centre
Dr Vektor Dewanto, Research Officer, UQ Gas and Energy Transition Research Centre

Citation

Lane, J. (2025). Long-term back-casting of wind & solar capacity factors for the ISP Renewable Energy Zones. Gas and Energy Transition Research Centre, The University of Queensland, Australia

Acknowledgements

The author would like to thank members of the *Analytics and Market Trends* team within the (then) Queensland Government Department of Energy and Climate, for advice on implementation of this project. Thanks also to UQ-GET staff (Andres Peredo Marquez; Ismael Khan) for coding support.

Disclosure

Researchers within or working with UQ-GET are bound by the policies and procedures of The University of Queensland that ensure research integrity is maintained (Responsible Research Management Framework Policy).

UQ-GET is funded by The University of Queensland and industry members (Arrow Energy, APLNG, and Santos). This project also drew on funding support from the Queensland Government, the Australian Gas Industry Trust, CleanCo Queensland Limited and CS-Energy Ltd.

Disclaimers

The information, opinions, and views expressed in this report are those of the author, and do not necessarily represent the opinions or views of The University of Queensland, UQ-GET and its constituent members, or other entities providing funding support for this research.

This report has not been independently peer reviewed.

Abstract

As Australia's National Electricity Market (NEM) becomes increasingly reliant on supply from wind and solar generation, its vulnerability to future weather variability will increase. To assess that risk, much of the energy transition modelling community relies on data published by the market operator (AEMO), which at the time this work was undertaken, covered 13 years (2010-11 to 2022-23) of wind and solar capacity factor (CF) variability. Although other analyses have illustrated that time-period may not be sufficient to cover the low-side risk from variable renewable electricity (VRE) generation droughts, there have been no alternative datasets developed that maintain alignment with AEMO's renewable energy planning zones.

This study addresses that gap, aiming to improve the application of weather-related uncertainty analysis within long-term transition pathway modelling. CF timeseries are produced for the NEM's renewable energy zones (REZ), calibrated to the AEMO CF data over their 13-year period, then back-cast over a longer timeseries (80 years, at 30min resolution). This is repeated using weather data from each of the BARRA-R2 and ERA5 reanalysis products.

The modelled CF show clearly that AEMO's CF data does not adequately capture the variability in VRE generation potential over that longer historical record. An example case study shows that, for each year of the transition through to 2044, relying solely on AEMO's data could potentially underestimate the NEM requirements for *peak-day* firming by ~30-60%. If gas-powered generation (GPG) continues to evolve as the NEM's primary *'option-of-last-resort'* service provider, as is currently anticipated by multiple planning studies, underestimating the need for gas supply to GPG (by that margin) could threaten future NEM resilience.

Key strengths and weaknesses of these novel CF datasets are illustrated, aiming to improve their application in applied uncertainty analysis of energy system transitions. The methodology chosen for this study is capable of (a) being rapidly updated when future AEMO data is released; and (b) incorporating other methodological improvements that would expand the scope of use cases for which the data is relevant.

Contents

Tables

Figures

Executive Summary

Project Overview

As the Australian east coast electricity system (the National Electricity Market - NEM) becomes increasingly reliant on supply from wind and solar generation, its vulnerability to uncertain future weather variability increases. To assess that risk, much of the energy transition modelling community relies on AEMO's published data for wind and solar capacity factor (CF) variability. At the time this work was undertaken, that AEMO data covered a 13-year period (2010-11 to 2022-23). Although other analysis has demonstrated that period may not be sufficient to cover the low-side risk from variable renewable energy (VRE) generation droughts, there have been no alternative datasets developed that maintain alignment with the NEM's renewable energy zone (REZ) boundaries.

This study helps address that gap, aiming to improve the application of weather-related uncertainty analysis within long-term transition pathway modelling. In particular, this study:

- Produces CF timeseries at the REZ-level that minimise deviation from the AEMO CF traces[a] over their 13-year period, then back-cast the CF over a longer timeseries (80 years, 30-minute resolution), using an approach that is compatible with the AEMO methodology.
- Provides the first REZ-specific assessment showing that AEMO's CF traces do not adequately capture the variability in variable renewable energy (VRE) generation potential, over that longer historical record.
- Demonstrates that underestimating future VRE resource variability could have material consequences for planning the infrastructure needed to ensure long-term NEM resilience, using a case study of gas-powered generation (GPG) as the NEM's supply *'option-of-last-resort'*.
- Documents key strengths and weaknesses of these novel CF datasets, to facilitate improved application of uncertainty analysis into the modelling of energy system transitions.
- Trials and documents methodology for generating CF over long time-series, in a way that facilitates rapid updates (when future AEMO data is released) and methodological improvements (to expand the number of use cases for which the data is relevant).

Recommendations for Planners and Policy Makers

❖ **AEMO's limited set of historical *weather-years* do not represent the extent of low-side risk in the NEM's wind and solar resource potential.** Multiple earlier years have 7-day, 30-day and/or 120-day periods of wind generation potential that are substantially lower than occurs during AEMO's 13-year period of CF data[b]. Planned revisions to AEMO's methodology will add the two most recent years to their suite of CF traces, but are not anticipated to extend them further back in time.

Variability in the wind CF is most pronounced for the May-August (winter) months in the southern NEM states, with the Queensland wind resource having the least inter-annual variability over the longer historical record. The extreme low-wind winters often occur simultaneously in multiple southern states. The 1940-1960 period provided the lowest aggregate wind potential. The limited available literature suggests that those earliest decades should not *prima facie* be discounted as un-representative of future possibilities. Further investigation would be needed to make more specific recommendations on this issue.

[a] CF *"traces"* is terminology used by AEMO to describe their published data on VRE resource variability. In this report, the terms '*CF data'* and '*CF traces'* are used interchangeably.

[b] as used for AEMO's energy system planning studies in 2024 and 2025

The solar CF show less inherent variability over the long term, though all seasons have earlier years where the solar resource drops below the range captured by the AEMO data. Although wind variability will be the largest overall contributor to winter VRE resource uncertainty, periods of unanticipated low solar output may still pose a consequential risk if they occur when wind generation is also low. Inter-annual variability in solar PV generation potential is greatest for Queensland, particularly in summer months, suggesting that additional analysis might be needed to ascertain risks in that state.

- **A case study on GPG planning challenges, demonstrates the potential importance of utilising a more extensive set of CF data for energy system planning.**

  Energy system planners expect GPG to be acting as the *option-of-last-resort (OOLR)* in the future, filling VRE supply gaps (particularly in winter) that exceed the capacity of a massive future fleet of batteries and pumped hydro. For it to perform that role, a wide range of modelling studies show that peak GPG capacity will need to increase substantially beyond its current level. However, planning the scale of that expansion is particularly challenging, as long lead times (multi-year to decadal) might be required to ensure that gas supply system (production, storage, transports) infrastructure is fit-for-purpose to meet the increasingly volatile demands of gas for GPG.

  A simplified method is used to estimate the potential scale of winter VRE shortfalls *over and above those* anticipated by the AEMO CF data. The analysis suggests that, for each year from 2030 to 2044, the need for peak-day *OOLR* firming (NEM-wide) could be ~30-60% higher than AEMO accounts for. Underestimating the need for GPG by such a considerable margin, could result in insufficient gas supply capability being available when and where needed. Constraining the ability of GPG to act as a reliable *OOLR* could pose a considerable risk to maintaining long-term NEM resilience.

  These NEM concerns would remain relevant, even should another technology evolve to displace GPG as the primary *OOLR*. Australia's energy transition planning process should therefore prioritise more systematic analysis on the scale, timing and location of future *OOLR* firming capacity that might be required to buffer for uncertain future VRE variability.

- **Increased transparency on the AEMO CF modelling process would improve the development of alternate CF datasets that provide complementary benefit to energy industry stakeholders and planners.** More robust and effective uncertainty analysis requires a much broader base of research effort, and would inherently benefit from trialling, comparing and contrasting the implications of using different datasets and modelling methodologies.

Key Modelling Conclusions

- **The ERA5 and BARRA-R2 reanalysis products were chosen to provide the weather data for the CF results developed in this project.** Neither Australia's Bureau of Meteorology (BoM) weather station data, nor gridded products that interpolate across observational records, could provide the necessary spatio-temporal coverage and resolution, across all weather variables required. The more commonly used MERRA-2 (global) reanalysis product was not used, as initial analysis showed that ERA5 and BARRA-R2 are superior at matching BoM observed data.

- **CF times-series at 30min intervals were developed for each REZ and each VRE resource category used in AEMO's ISP-2024.** Consistent with the data published by AEMO, the modelled CF data covers solar PV (single-axis tracking), onshore wind (wind-high; wind-medium, and offshore wind (fixed platform; floating platform). CF data was generated separately from each of the ERA5 (1941-2023) and BARRA-R2 (1981-2023) reanalysis products.

- **The modelled CF are able to recreate core aspects of variability in the AEMO CF data, proving useful to assess the risks of VRE resource variability over a long-term dataset**. Strengths and weaknesses of the two reanalysis-based products are compared and explained. One key limitation is their suppressed estimation of solar CF variability over weekly to longer-term timeframes, however that is not expected to influence the conclusions drawn in this study.

- **For applied modelling of NEM transitions, the preferred choice of CF product may depend on which electricity system risk factors are being targeted in the analysis.**

  Overall, there is very little difference between the sets of CF data derived from the different reanalysis products, with neither proving to be the 'best' in all regards. ERA5 was considered suitable for the GPG analysis example provided here, because (a) the priority was on using the most extensive (longest) CF dataset possible, and (b) the most notable limitations with the modelled CF were not considered influential to the scope of analysis. However, that may not be the case when considering different risk perspectives.

  Users should be cautious about mixing across different CF products within a single analysis of energy system risk, particularly if they require high fidelity at sub-daily scales. The correlation across the two modelled CF datasets (and for comparisons with the AEMO CF) are notably weaker at the hourly scale. Much better correlations are achieved at daily or longer timescales.

  The wind CF in both products are calibrated well to the AEMO traces, and provide long-term daily trends that are well correlated with each other. Their relative strengths vary across location, season and wind regime. For example, while ERA5 provides a slightly better overall fit to the AEMO benchmark in most REZ, for some REZ the BARRA-derived model is superior at matching the AEMO CF distribution for lower wind periods in the critical winter risk period.

  For the solar CF, there are more pronounced differences across the two reanalysis products. Both are well calibrated to the yearly and seasonal inter-annual means of the AEMO data, though underestimate the variance in that AEMO benchmark. That suppressed variance likely results from discrepancies in the underlying reanalysis estimates of cloud cover and irradiance. The modelled CF (particularly from BARRA-R2) are therefore prone to underestimating the depth of solar PV shortfalls. Conversely, the CF based on BARRA-R2 are superior at representing solar generation potential in the critical summer afternoon period, when NEM supply-demand balances can be under extreme stress.

- **Improved and expanded CF development could deliver substantial benefits to electricity and gas sector stakeholders. This report suggests multiple opportunities to greatly improve the utility of such CF products**: (i) Minor methodological modifications to reduce discrepancies with the published AEMO CF data; (ii) Additional tool development to facilitate more effective use of these CF in energy system modelling; (iii) More extensive consideration of weather uncertainty, to improve the statistical robustness of CF application in applied uncertainty analysis; and (iv) Extend the scope to include rooftop solar PV and hydro generation.

1. Motivation

The predominant vision for deep decarbonisation of Australia's east coast electricity system (the *NEM*[c]), requires an unprecedented level of reliance on variable renewable electricity (VRE) generation.[1–4] Accommodating such large contributions from variable supplies will require major changes from the historical approach to planning and operating the NEM market and infrastructure.[5–8]

AEMO's[d] Integrated System Plan (ISP) modelling studies have an important role in the NEM infrastructure planning process. The latest release (ISP-2024) provides three distinct scenarios, all involving the extensive shift from a coal-dominated to VRE-dominated system, though differing in the pace at which that occurs. The ISP's prominent *'Step Change'* scenario sees VRE growth accelerating rapidly, becoming the dominant NEM supply source by the 2030s.[3] Their scenario results also illustrate the urgency of new investments that will be required if Australia's decarbonisation objectives are to be met.

Regardless of whether the ISP pace of *future* change is realised, the NEM has *already* shifted to a level of reliance on solar and wind infrastructure that creates vulnerabilities. Recent years have seen an increasing number of periods where VRE dependencies have created stress on NEM operational resilience.[9] Furthermore, VRE growth is *already* undermining the financial viability of the existing coal generation fleet, hastening the retirement decisions of privately owned plant[10,11], and arguably raising a barrier to the entry of new, lower-carbon dispatchable generation technologies.

As the NEM's reliance on VRE supply grows, its vulnerability to uncertain future weather variability increases. The policies, market redesign and supporting infrastructure needed to compensate for that vulnerability, all require planning well in advance; and the effectiveness of that planning will depend on how well future uncertainties have been anticipated. This is a particular challenge for planning the supporting infrastructure (e.g. transmission, batteries, pumped hydro, fully dispatchable generation), given much of the decision making has to happen in the very near term, without a high degree of confidence on how other aspects of the NEM transition will pan out. Commitments to that infrastructure are capital intensive, hence difficult to reverse within the economic lifetime (typically 20-30 years) of new facilities.

Integrating robust uncertainty analysis into the NEM's infrastructure planning will therefore be critical, to accommodate the speed of VRE uptake and reduce the likelihood of undesirable transition path dependencies. International studies have demonstrated how transition scenario modelling can be highly sensitive to assumptions about future weather variability.[5,12] Assessing the risk of future electricity supply shortfalls therefore requires a focus on probabilistic outcomes, with the use of 'typical' VRE resource potential estimates not being suitable.

For the ISP-2024, AEMO provided multiple scenarios for future weather variability, based on hypothetical VRE capacity factor (CF) estimates across 13 different *weather-years* (2010-11 to 2022-23). That CF data is published for each Renewable Energy Zone (REZ) considered in the ISP, derived from a mix of modelling and empirical performance data.

However, the published AEMO CF data may be too limited for robust assessment of the implications of uncertain future weather variability. Multiple independent analyses have concluded that AEMO's 13 *weather-years* do not likely cover the low-side risk from VRE generation droughts, with the potential for larger VRE shortfalls evident in years prior to AEMO's *weather-year* period.[13–15] Unfortunately, those prior studies provide limited guidance for others wishing to adopt an alternative to AEMO's data. For example, none provide a systematic set of alternative VRE resource potential estimates at the level of AEMO's Renewable Energy Zones (REZ), nor has there been any public critique of the best datasets and methodology to use for that purpose.

[c] The National Electricity Market (NEM) term is used to refer both to the physical electricity system (spanning Queensland Qld), New South Wales (NSW), Victoria (Vic), South Australia (SA) and Tasmania (Tas), and the market used in system operations.

[d] The Australian Energy Market Operator (AEMO) manages NEM market operations on a day-to-day basis, but also has a separate function engaging in strategic planning for the NEM's physical and market systems.

Study Objectives

This study generates and analyses novel long-term (40-80yr) capacity factor (CF) timeseries for centralised wind and solar PV generation, addressing key gaps in the information needed to improve the application of weather-related uncertainty analysis within long-term transition pathway modelling.

Specific objectives were to:

1. Produce CF for each REZ in the AEMO ISP-2024 study, minimising deviation from the AEMO CF traces over their 13-year period; such that the longer time series provides a back-cast of CF trends using an approach compatible with the AEMO methodology.
2. For REZ-level modelling, assess whether AEMO's 13 weather-years are representative of low VRE resource risk over that 80-year historical period.
3. Provide a dataset that can be easily used by industry and researchers, with transparency over its strengths and weaknesses.
4. Develop a methodology for generating CF over long time-series, in a way that (a) enables rapid updates, should AEMO subsequently modify their own methodological approach; and (b) can accommodate a broader set of modifications, so as to expand the number of use cases for which the data is relevant.
5. Explore the potential importance of utilising an expanded CF dataset, using a case study on the implications for planning the firming infrastructure needed to ensure NEM resilience over the long term.

---

2. Methodology

To meet the objectives outlined above, this study's modelling approach was guided by the following principles:

i. **Utilise publicly accessible data and modelling algorithms**, to maximise transparency and repeatability of the work. In that regard:
   - Chosen weather datasets should provide users (of the modelled CF) with the option of maintaining internal consistency in the spatio-temporal relationships across multiple weather variables; and
   - For modelling power output, a priority was given to the use of open-source models that utilise and respect core physical and engineering principles; as such models can easily be critiqued and adjusted, should modelling preferences change in the future.

ii. **Maintain consistency with AEMO's approach to technical and technology assumptions**, albeit constrained by the limited public transparency over the details of their methodology. This study did *not* seek to test or demonstrate "improvements" to the way AEMO estimates wind and solar resource potential[e].

iii. **Calibrate the modelled CF results to give a better statistical match to AEMO's published CF traces.** Where appropriate, multiple alternative technical assumptions were trialled, to select the approach that minimises disparities between the modelled and AEMO CF data. Remaining disparities were then further reduced using a statistical error correction process.

iv. Apply the calibrated model to the full historical dataset available in the reanalysis products, producing long-term CF time-series at 30min resolution.

[e] other than through extending the choice of historical years that are included

2.1 Data for weather variable inputs

Multiple datasources were reviewed for their ability to provide sufficient spatio-temporal consistency across multiple weather variables, considering the following requirements: (i) Strong and representative spatial coverage across all key (current and future) regions of VRE deployment; (ii) Inclusion of all key weather variables needed for energy systems modelling; and (iii) Long-term weather history at hourly resolution, across all weather variables and all locations.

Two categories of data were considered but not utilised – weather station data from the Australian Bureau of Meteorology (BoM); and high-quality gridded datasets based on statistical interpolation across the network of observation stations. Although these likely provide the most 'accurate' available representation of Australian conditions, neither were considered to have sufficient spatial and/or temporal coverage across sufficient weather variables, to meet the requirements for this study.[f] Further comment on available Australian weather data is provided in Appendix A.

Reanalysis products

Historical weather data for this study were taken from multiple '*Reanalysis*' products, that provide gridded data across large regional systems, typically at sub-daily scale. Reanalysis products use climate system models to recreate past climate observations at global and large-regional scale, over a long-term historical record. Table 1 outlines key characteristics for each of the reanalysis products considered.

Reanalysis datasets are often used for deriving historical CF traces for wind and solar PV, across most major electricity systems of the world.[17–22] The MERRA-2 reanalysis product has been one of the most commonly adopted, likely in part because derived CF traces (for a limited number of years) have been made easily accessible via the Renewables Ninja website[g]. MERRA-2 has also been the most commonly used reanalysis dataset in prior CF analysis for Australian energy systems.[13,14,23–29]

This study instead uses the global ERA5 and Australia-focussed BARRA-R2 reanalysis datasets, rather than the more commonly used MERRA-2 product, for the following reasons:

- Both provide an equal or longer historical record, at a much higher spatial resolution than is available with MERRA-2. Multiple studies have identified that low grid resolution is a weakness for modelling wind power generation, given wind patterns can be highly spatially heterogeneous.[17,18]
- Analysis in other jurisdictions tends to conclude that wind CF derived from ERA5, rather than MERRA-2, are superior at replicating the performance of actual wind farms.[18,19] The available Australian analysis shows more mixed findings in this regard.[26]
- Both ERA5 and BARRA-R2 provide wind speed estimates at a range of elevations (above ground level) that is more appropriate for contemporary wind turbine operations.
- Unpublished UQ analysis showed that ERA5 and BARRA-R2 are (in most cases) superior at matching BoM observational data for variables and regions relevant to NEM energy systems. That conclusion is consistent with other more general analyses, that show MERRA-2 tends to be less skilful at recreating Australian weather observations.[16,30]
- AEMO's methodology for developing wind-CF previously utilised ERA5, with future versions to instead adopt BARRA-R2[31].

Appendix A provides a list of the specific variables used as the power modelling inputs.

2.2 REZ boundaries

CF timeseries are produced for all REZ regions as defined in the Draft release of the ISP-2024. The Final ISP-2024 release involved some changes to offshore wind boundaries, though that affected only a few

[f] BoM's own critique[16] supports the conclusion that these products have limitations for analysis of broad-scale and long-term trends, when high spatio-temporal detail is also required.

[g] see https://www.renewables.ninja/

REZ that collectively contributed very little to the final infrastructure build scenario results. Two sets of CF results (N10, N12) were excluded in this study, though this has no impact on the comparative analysis provided in this report, as neither feature in AEMO's infrastructure solutions for the ISP - see Appendix A for more details.

Table 1: Key characteristics of the reanalysis products considered for this study

Reanalysis product		**MERRA-2**	**ERA5[h]**	**BARRA-R2**
Source		NASA (USA)[32]	ECMWF (Europe)[33,34]	Aus Bureau of Meteorology[35]
Spatial	*coverage*	global	global	Aus, Sth Pacific, SE Asia
	grid size	50 x 60km	30km	12km
Temporal	*coverage*	1980 - present	1940 - present	1979 - present
	timestep	Hourly	Hourly	Hourly
Fixed-height elevations (for wind speed data)		Surface; 50m	Surface; 100m	Surface; 50m; 100m; 150m; 200m
Key strengths		Widely used for power systems analysis	Longest time series; Often identified as the more accurate *global* product at matching observed data for wind resources. Superior fit to BoM observed data. Utilised by AEMO for their wind-CF used in this study.	Locally derived, nested inside the global ERA5; Highest spatial resolution; Best set of windspeed elevations. Superior fit to BoM observed data. Will be utilised for developing wind-CF in future AEMO studies.

2.3 Modelling Approach

The wind and solar CF modelling largely followed the same overall methodological steps, albeit with key differences that are outlined in each of the subsections below. Table 2 provides a summary of key similarities and differences.

To the extent possible, steps #1-4 attempt to maintain consistency with the principles and approach of the AEMO methodology for modelling CF. However, for all stages of the workflow, insufficient published information could be found to ascertain key details of the AEMO method. Key assumptions were therefore tested using detailed sensitivity analysis, though this study did not attempt an exhaustive assessment of all possible methodological choices. Future iterations of this modelling will expand on those methodological investigations, aiming to provide greater fidelity to the published AEMO data (see Section 3.4).

1. Locational screening

Each REZ boundary contains multiple reanalysis grid cells, with each grid cell processed separately in the subsequent power modelling step.

For the onshore wind and solar PV categories, grid cells were screened out to avoid locations with likely social or environmental constraints on development. The application of land-use exclusions followed the methodology developed in the Net Zero Australia study[2], which account for a similar set of exclusion categories to those listed by AEMO, but also rule out development on high value irrigated and rain-fed cropping lands. Although AEMO only explicitly adopts such an approach for their onshore wind modelling, their methodology for solar PV is such that land availability constraints are likely to be accounted for indirectly.

[h] ERA5 data was taken from the Copernicus Climate Change Service. Neither the European Commission nor ECMWF is responsible for any use that may be made of the Copernicus information or data it contains.

Grid cells in onshore REZ are further classified into the *Wind-High (WH)* or *Wind-Medium (WM)* categories using quantile-based bins, in accordance with the approach described by AEMO. The *WH* category includes grid cells in the top 15th percentile of time-averaged CF, as calculated for each grid cell over the 13yr AEMO *weather-year* period; whereas grid cells falling between the 15th–40th percentiles are included in the *WM* category. This allocation process is applied independently for each of the ERA5 and BARRA-R2 data, meaning that different grid cells might be chosen for the WH (or WM) category, depending on which reanalysis dataset is being used.

For offshore REZ, grid cells are allocated into two categories based on thresholds specified by AEMO - *Fixed-Platform* (FX) for average sea-depth < 70m; and *Floating-Platform* (FL) for depths >70m.

Because of the large reanalysis grid cell size (particularly for ERA5), the above steps were used to generate inclusion "weightings" for each grid cell in each wind and solar PV category, so as to avoid screening out entire grid cells because of a small, partial overlap.

Table 2: Overview of the modelling steps to produce wind & solar CF

Step		Wind	Solar PV
(1) Locational screening		Exclusions for social-enviro constraints. Resource quality allocation by onshore wind category (*WH* vs *WM*). Spatial data used to assign grid cells by offshore grid category (*FX* vs *FL*).	Exclusions for social-enviro constraints.
(2-3) Power conversion model	Model	windpowerlib[36]	pvlib[37]
	Config	Power curves to represent Class I, II, III turbines; smoothed to windfarm-level. Adjustment for wake losses.	Single-axis tracking, with contemporary panel & inverter specs
	Key sensitivity tests	Turbine class & hub-height chosen (by REZ) to give best statistical match to the AEMO traces.	Models for irradiance decomposition & transposition chosen to best match diurnal profiles.
(4) CF calculation at REZ level		Average across grid cells, for each wind category (WH, WM, FX, FL)	Average across grid cells
(5) Statistical correction		Minimise discrepancies in the CF mean and variance, by adjusting wind speed profiles for each grid cell.	Minimise discrepancies in the CF mean, by scaling the CF time-series using seasonally varying scaling factors.
		For each wind category in each REZ, a pair of correction scalars (α, β) are chosen, based on comparison (model vs AEMO) over 13yrs of hourly CF data.	For each REZ, a set of weekly correction parameters (γ_w) is chosen, based on comparison (model vs AEMO) over 13yrs of daily-avg CF.
(6) Final output		Interpolated to 30min resolution.	Interpolated to 30min resolution.

2. Power model configuration

The chosen power generation models (windpowerlib; pvlib) are taken from readily accessible, open-source software, both considered best-practice for modelling long-term CF if using reanalysis data and open-access tools.[i] Both provide considerable flexibility in how the technical models are configured.

For this study, the objective was to choose a set of engineering-based methods and assumptions that strike a balance between (a) maintaining consistency with the methodology used by AEMO; (b) reducing

[i] For PV power modelling, AEMO uses the SAM software developed by the US National Renewable Energy Laboratory (NREL) – however the available literature suggests that model choice is not of itself an important source of uncertainty, as SAM and pvlib will give similar results if the inputs are equivalent. For wind power modelling, AEMO uses a mixture of machine learning and engineering models, though doesn't document what they use for the latter.

the majority of discrepancy between the modelled results and AEMO's CF traces for the ISP *weather-years* period; and (c) allowing consistent application across all REZ. Note that neither the wind nor PV modelling accounts for performance loss over time.[j]

Key details on the separate wind and solar power modelling approaches, are outlined below.

Wind

Indicative power curves were developed for Class I, II and III turbines[k], based on a review of turbine-specific power curve data from *'The Wind Power'* database[l]. The normalised, turbine-level curves are shown in Figure 1a.

The following two steps then helped to reduce the error between the modelled results and the benchmark AEMO CF traces:

- The reanalysis-derived wind density (at hub height) is modified to account for intra-farm wake losses, using the default function in windpowerlib.
- The turbine-specific power curves (Figure 1a) are converted to windfarm specific power curves (Figure 1b), accounting for the variation in wind-speeds that would be seen across different turbines in the wind farm (at any given point in time), and across different minutes within each hour. This adjustment assumes those heterogeneities are normally distributed, applied using the default parameters available in windpowerlib.

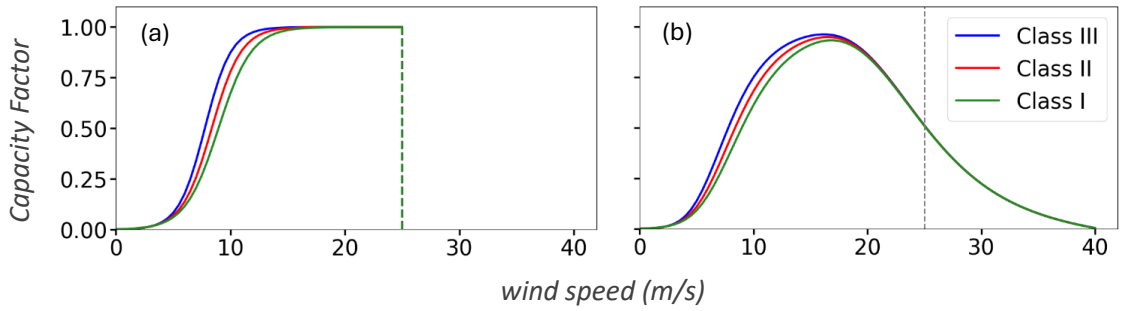

Figure 1: Windspeed-Power curves used for the modelling

(a) Turbine specific power curves used for each turbine 'class'; (b) Aggregate Windfarm power curves, after allowance is made for a normally distributed range of wind-speeds that present to any given turbine at any specific point in time.

Solar PV

The two most critical assumptions that were tested, relate to the choice of decomposition and transposition models that get applied to the raw irradiance data. The adopted models provided the best fit to the diurnal shape of the AEMO CF traces, and are consistent with literature best practice for assessing long-term CF variability.

- The DISC model[38] was used to decompose the reanalysis GHI estimates into DNI and DHI terms.[m] The native DNI estimates of ERA5 and BARRA-R2 were not utilised, as incorporating them directly into the modelling gave far inferior results.
- The decomposed irradiance terms are then transposed into Plane-Of-Array irradiance using the Perez model[39], accounting for panel orientation and operation of the tracking system.

[j] AEMO provide no documentation that would inform assumptions on VRE performance degradation. Should AEMO have intrinsically included performance degradation in their own methodology, then this will indirectly be accounted for using the statistical error correction process adopted for this study.

[k] This turbine classification is taken from the wind industry's IEC 61400 standard, used here to provide an indicative illustration of what is realistic in high-wind (Class I) to low wind (Class III) regimes.

[l] see https://www.thewindpower.net/index.php

[m] GHI = Global Horizontal Irradiance; DNI = Direct Normal Irradiance; DHI = Diffuse Horizontal Irradiance

Chosen assumptions for the panel tracking system (horizontal hub running north-south; max. tracking angle of ±45°; backtracking enabled) represent a mix of (a) maintaining consistency with common practice in the regional-scale modelling literature; and (b) providing the best fit to the AEMO CF traces.

The DC power output calculations account for the loss of efficiency at high temperatures; then the inverter process is modelled to estimate the final AC power output.

3. Future technology configuration

In the absence of clear documentation on the AEMO methodology, exploratory analysis was required to determine critical assumptions on physical technology configuration. The following subsections describe the approaches that were chosen to reduce error between the modelled and AEMO CF values.

Note that the possibility for future technological evolution, or future efficiency improvements with current technology, were not considered in this study. From the AEMO documentation available, it does not appear that they account for these issues.

Wind

AEMO's methodology descriptions outline that: (a) They employ different methodologies for REZ that do and don't have existing wind farms; (b) For REZ with existing wind farms and sufficient operational data history, the CF are (at least in part) informed by machine learning algorithms applied to that empirical operational data; and (c) When hypothetical future wind farms are being modelled, weather data from ERA-5 is used as inputs to an engineering-based power generation model.

Unfortunately, no AEMO documentation was identified that clarifies which approach was used for each REZ. Furthermore, it was not clear what assumptions were used for key technology parameters (turbine hub-height; power curve) that can strongly influence the wind power modelling results.

Because of that uncertainty, an initial screening step was undertaken using ERA5 reanalysis data, to determine an appropriate combination of hub-height and wind-farm power curve (see Figure 1) for each REZ. Appendix A lists the chosen assumptions.

Solar PV

AEMO only provides (and uses) REZ-level CF traces for the single-axis tracking configuration of solar PV generation. Assumptions for the tracking specifications are described above (Step #2). The modelling also assumed the use of panel and inverter types that were considered consistent with best-practice at the time this work was undertaken.

4. CF calculation at REZ-level

Using the power models described above, CF time-series for each wind and PV category were generated for each grid cell within the REZ.

The REZ level CF timeseries was than calculated by aggregating across all the grid cells, on a weighted average basis. That weighting process incorporates the *'Locational Screening'* issues described above, namely (a) the possibility of land-use constraints, and (b) the allocation to different wind categories.

5. Statistical correction

For the final step, statistics-based approaches were used to reduce any residual error between the modelled CF and the benchmark AEMO CF traces over the 2010-11 to 2022-23 (13-year) period. This was undertaken separately for each of the CF products derived from ERA5 and BARRA-R2.

Wind

The following approach was implemented independently for each of the four different wind CF categories (*WH*, *WM*, *FX*, *FL*).

For each REZ, a 2-term error correction approach was set to adjust the mean and variance of the input wind-speed time series at the modelled hub-height (Equation 1). The chosen error correction

parameters (α, β) were computed using bi-level optimisation to minimise the difference (from the benchmark dataset) in the mean and variance of the CF time series across the entire 13 years used in the AEMO data.

$$ew^*_{g,t} = \alpha_r \cdot ew_{g,t} + \beta_r \quad [\ 1\ ]$$

where: $ew_{g,t}$ *is the reanalysis-derived, hub-height estimate of effective wind speed (corrected for air density & wake-loss effects) in grid cell g, at time t*

$ew^*_{g,t}$ *is the adjusted (post-correction) wind speed, at time t*

α_r, β_r *are the error correction terms for REZ r*

This approach is consistent with common practice in research literature[21], where error-correction approaches aim to improve both the mean and variance of modelled power output by adjusting wind-speed inputs rather than the final CF values. Adjusting the power model inputs is preferred, because of the complex non-linearities involved in converting wind speed to power output (as illustrated by the power curves in Figure 1). A complementary Australian study adopts a similar approach to that used here, aggregating existing wind farms by state then tuning both error correction terms (α, β) at that state-aggregated level.[14]

Solar

The solar PV error correction process was applied directly to the calculated CF values. Multiple approaches were explored, with the following two-step method being adopted: (i) Weather input data for the late afternoon period (from ~2:30pm) were shifted forward in time by 30min, to compensate for an error introduced by relying on hourly timestep data; then (ii) a 1-term error correction was then applied, based on the ratio of daily-mean CF, as per Equation [2].

$$CF^*_{r,t} = \gamma_{r,w} \cdot CF_{r,t} \quad [\ 2\ ]$$

where: CF_t *is the uncorrected, reanalysis-derived capacity factor for REZ r, at time t*

$CF^*_{r,t}$ *is the corrected series of CF*

$\gamma_{r,w}$ *is the ratio (AEMO-CF / modelled-CF) of mean-daily-CF, for REZ r, with one coefficient specified for each calendar week (w)*

The error correction terms (γ_w) are derived on a weekly basis, to account for the strong (non-random) seasonal differences in PV output. Applying a single aggregate set of correction terms would overstate the variability of PV output in winter periods and understate that variability in summer periods.

Unlike for wind modelling, there is comparatively little literature exploring approaches to error correction for long-term solar CF estimation – the formative paper by Pfenninger and Staffell (2016)[22] provides the closest template to our work, adjusting PV modelling outputs (CF traces) to better match a regional aggregate benchmark. From the limited Australian analyses available, one study highlights the need for (but doesn't implement) dynamic error correction[20], while the other doesn't document whether an error correction algorithm is used[14].

6. Final output

For both wind and solar, the CF results are disaggregated to a 30min timesteps using a cubic spline interpolation, to match AEMO's 30min resolution for CF traces.

2.4 Analytical Approach

The CF modelling is undertaken at REZ-level, though this report primarily presents illustrative results using three specific regional definitions. The Q8 REZ is used as an example of the direct CF results, chosen because it is one of the largest REZ (across wind and solar generation) in the future ISP

scenarios. Queensland and Victorian state-aggregate regional groupings are also provided, to illustrate the implications of climatic differences across the NEM. Appendix B provides results for other states.

Solar results for Tasmanian REZ were generated but are largely omitted from this analysis, because the ISP-2024 *Step Change* scenario does not involve any buildout of solar PV in that state.

All time references in this report are on a calendar-year (not financial-year) basis, unless indicated otherwise. Summer-season results are reported to the year in which the summer ends, e.g. results reported as "summer 2019" are for the summer period ending in Feb 2019.

Aggregation across REZ & across VRE categories

Wind CF results are shown as an aggregate across all relevant wind categories (*WH*, *WM*, *FX*, *FL*) for the region in question.

Unless specified otherwise, all CF aggregation (across regions and/or VRE categories) is done by capacity-weighted average, with the weights set at the REZ-specific installed capacity results for the final year (2052) of the ISP Step Change scenario[n]. That choice of weighting factors provides some perspective on how the modelled CF results would influence electricity system modelling over mid-century timeframes, recognising that the expected future VRE buildout is not evenly spread across REZ.

Temporal aggregation and grouping

Rolling averages are applied to the CF time-series in various ways throughout this report. In all cases, the averages are centred around the date that is shown in the analysis.[o]

Seasonal groupings are used in some analysis, dividing the year into three distinct 4-month periods: *Summer* (Nov-Feb), *Winter* (May-Aug) and a *Bridge* (Mar-Apr, Sep-Oct) season. The rationale for using these non-traditional groupings was two-fold. For solar PV, the four monthly periods provide greater symmetry around the summer and winter solstices, and therefore a more evenly distributed range (within each seasonal grouping) of critical time-varying factors (clear sky irradiance; solar zenith angles). For wind, prior modelling-based analysis[13] and recent years' experience[40] show that low wind periods in May can contribute significantly to the overall challenge of NEM supply-demand balancing over winter.

Comparison with AEMO CF traces

The modelling results (referred to in this report as the *'modelled CF'*) are benchmarked against the CF traces published by AEMO in their Draft ISP-2024 release (*'AEMO CF'*), so as to maintain consistency with the definition of the REZ regional boundaries (also taken from the Draft ISP-2024).

The comparisons are mostly provided on a seasonal or calendar year basis, hence not using the financial-year nomenclature used by AEMO in their published CF traces. Where necessary, the comparison period was reduced to less than the full length of the AEMO data to ensure that only full 4-monthly seasonal periods were considered.

To enable a direct comparison between the modelled and AEMO CF time-series, the AEMO CF traces were also adjusted to compensate for time-series modifications made in the AEMO methodology. Although AEMO's CF traces are based on the historical record, they are published as datasets to be used for future scenario years. Those published datasets involve the date-stamps for each year being shifted forwards or backwards by up to 3 days, so as to maintain consistency in the alignment of weekdays and weekends. That weekday/weekend distinction is important to modelling electricity demand, hence AEMO applies this shift to their VRE CF traces in order to maintain spatio-temporal relationships across the weather dependent aspects of both supply and demand.

[n] Installed Capacity results are taken from the AEMO results for the Optimal Development Path of the Step Change scenario, in the Final ISP-2024 release.

[o] For example, a 7-day rolling average attributed to the 10th July provides CF averaged over the period of July 7th-13th.

Multiple analyses are provided that compare how well the two modelled CF products (from ERA5; from BARRA-R2) match the AEMO-CF data. Superior performance in those tests implies a better fit to the benchmark, but not necessarily that either one is more accurate at representing real world conditions. Further comment on this is provided in the *Wind* and *Solar* subsections of Section 3.3.

2.5 Case study

Section 3.3 presents a short case study to explore the potential significance of utilising CF modelled over a longer historical record, for the energy system planning process.

The case study focus is on understanding future requirements for the *OOLR* supply, a burden expected to increasingly be met by gas-powered generation (GPG). The analysis narrows in on the uncertainty over, and challenges of planning for, the new gas supply infrastructure (production; storage; transport) that would be needed to ensure GPG can adequately perform its role in AEMO's ISP scenarios.

For this, the modelled CF are combined with additional data taken from AEMO's 2025 Gas Statement of Opportunities (GSOO) report.[41] The GSOO is AEMO's annual planning study that assesses near to medium-term risks with gas supply in the east coast gas market. It also provides the highest fidelity information available publicly, on the nature and scale of future supply shortfalls for the NEM, once the capabilities of VRE, hydro, storage and demand-side response are exhausted.

The case-study analysis modifies the default approach to the capacity-weighted averaging of CF results. Here, the weights for each annual time-step use the ISP's VRE capacity mix (by technology, by REZ) for that particular scenario year. The infrastructure capacity results are again taken from the *Optimal Development Path* of the *Step Change* scenario.

Other key analytical steps are outlined in the case study summary (Section 4).

3. Findings

3.1 Variability in the AEMO CF traces can be re-created

The analyses presented in this section highlight that CF modelling using accessible datasources and models, can provide CF traces for the 2010-11 to 2022-23 period that match key aspects of the variability within the published AEMO data.

Table 3: Statistical comparison (model vs AEMO) of the CF results, for the 2010-11 to 2022-23 period.

For each metric, the 10th percentile and 90th percentile *(p10/p90)* of the REZ-specific results is shown – for wind, these metrics are calculated across all onshore (WH, WM) and offshore (FX, FL) categories. Bias is the difference *[model – AEMO]* of CF means. For the variance indicators (Std Dev; p10-p90 range), ratios are calculated as *[model / AEMO]*. Pearson correlation coefficient and root-mean-square error (RMSE) are shown for comparisons of the modelled hourly CF, also for daily- and weekly-averaged CF.

		Bias	ratio of…		correlation			RMSE		
			Std Dev.	p10-p90	hourly	daily	weekly	hourly	daily	weekly
Wind	ERA5	-0.001 / 0.001	0.99 / 1.00	0.96 / 1.00	0.79 / 0.93	0.84 / 0.95	0.86 / 0.95	0.10 / 0.19	0.07 / 0.13	0.03 / 0.07
	BARRA-R2	-0.001 / 0.001	0.99 / 1.00	0.96 / 1.00	0.76 / 0.89	0.85 / 0.93	0.88 / 0.95	0.13 / 0.21	0.08 / 0.14	0.04 / 0.07
Solar	ERA5	-0.001 / 0.001	0.84 / 0.92	0.81 / 0.90	--	0.86 / 0.93	0.94 / 0.98	--	0.04 / 0.06	0.02 / 0.03
	BARRA-R2	0.000 / 0.002	0.76 / 0.88	0.71 / 0.87	--	0.86 / 0.93	0.93 / 0.98	--	0.05 / 0.06	0.02 / 0.03

The modelled CF have a strong statistical fit to the AEMO CF traces, on the basis of mean and variance (Table 3). The range of REZ-specific results shown here (10th percentile / 90th percentile) indicates that the wind model performs well for the majority of regions. For the few poorly fitting outliers that fall outside the range shown, the discrepancies might be explained by occasional flaws in the choice of technical modelling parameters used in this study, given it's unclear which REZ utilise empirical wind farm performance data under the AEMO methodology. The quality of fit for the uncorrected models is quite different across the two different reanalysis products (Appendix B), however Table 3 shows that the error correction step (#5 in section 2.3) eliminates most of that difference.

The CF modelled from ERA5 show a slightly better correlation with the AEMO benchmark, though this varies from state to state. Consistent with other international analysis[19], the correlation (and therefore RMSE) is weaker at the hourly level, but improves considerably when the results are aggregated on a daily and weekly basis (see also Figure 15).

The quality of fit for the solar CF is also good, though weaker than for the wind modelling.[p] For both the reanalysis-based models, the error correction process eliminates most of the bias. However, both also underestimate the variance in the AEMO solar CF traces, with the CF from BARRA-R2 being notably worse (than ERA5) in this regard.

The following sub-sections explore the effectiveness of the modelled CF in more detail. For simplicity, the results presented here are mostly for the ERA5-derived modelling. When there are important differences, results are also presented for the modelling with BARRA-R2 (also see Appendix B).

The modelled wind CF provide a strong match to the AEMO benchmark

Figure 2 illustrates that the correlation improves at state-level (compare Q8 vs Qld) but varies across states. That latter finding is unsurprising, given the uneven spread of existing wind farms means that some states are more likely (than others) to be affected by discrepancies in the weather data and wind technology assumptions used in this study.

[p] Hourly-resolution statistics are not provided for solar PV, to avoid the statistical comparison being distorted by the (predictable) night-time zero values. Figure 14 and Figure 15 provide some hourly resolution analysis for solar PV.

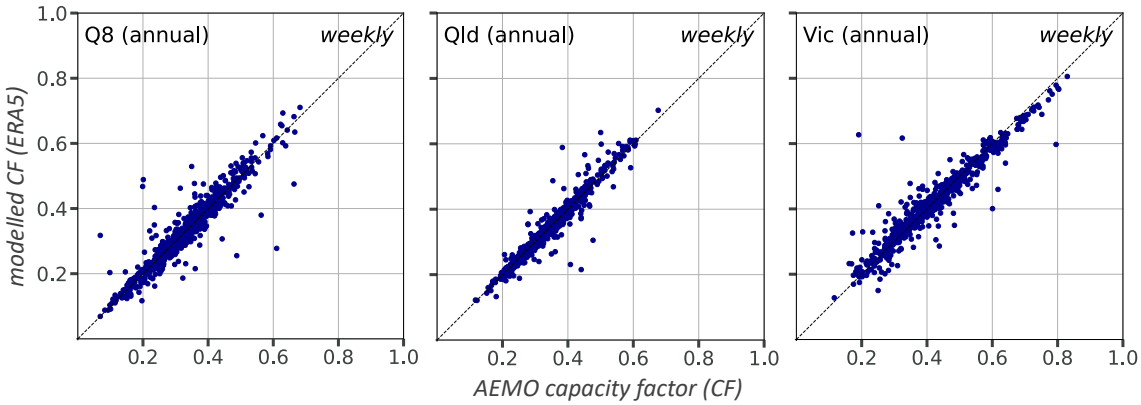

Figure 2: Comparison of modelled results vs AEMO CF over 2011-23, for weekly-avg wind CF.

Although the daily-level correlations still show some discrepancies (Table 3; Figure 15), Figure 3 shows that the modelling methodology recreates well the distribution of daily-average CF results, capturing key variations in the nature of the wind resource across seasons and regions. Both reanalysis models perform well across the full distribution in most locations, though the choice of which gives the best fit does vary by REZ. For the summer months, ERA5 generally provides a superior fit in southern states, and for Queensland during low summer wind periods. For the winter months, the ERA5 model tends to outperform BARRA-R2 in matching the AEMO distribution at higher levels of wind power output, whereas there are some southern REZ where BARRA-R2 gives the better fit for lower wind CF.

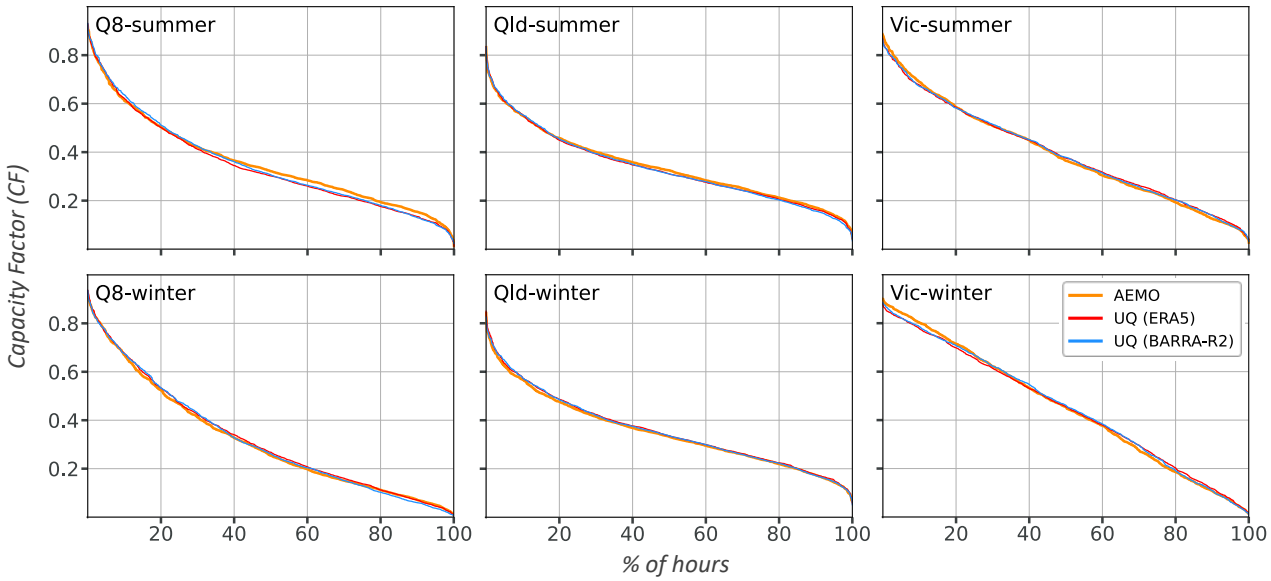

Figure 3: Generation-duration curves for daily wind CF (2011-2023), comparing both reanalysis models with AEMO.

Figure 4 utilises a different approach to demonstrate that the model results also match the spread of seasonal variability in the AEMO CF, and again this finding holds across all states with their substantially different wind profiles (see Appendix B). The plots compare 30-day trends across the modelled-CF and AEMO-CF, showing for any given stage of the year, the lowest and highest (30-day) outcomes across the 13-year comparison period.

Because of the good distributional and seasonal fit, the 7-day-average trend in the modelled CF is consistent with the AEMO traces, matching the variation across the year. Figure 5a provides example results for 2022 - noteworthy because it was a year when low VRE availability made a small but marginally significant contribution to a winter period of extreme NEM supply-demand stress[42].

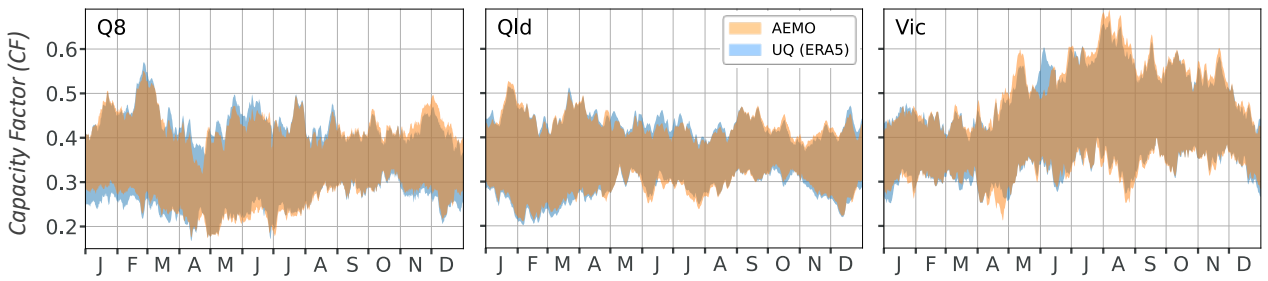

Figure 4: Seasonal spread of the aggregate wind-CF across 2011-2022, comparing modelled vs AEMO results.

For each time-series (modelled; AEMO) a 30d rolling-avg is applied; then for each calendar day, the min/max CF from any year is obtained.

By plotting the difference between the modelled and AEMO-CF across each year, Figure 5b highlights that most of the comparative discrepancies occur at the same times in each year. The errors are consistently much greater during periods that appear to coincide with public holidays (late Jan; March/April; mid-June; late Dec) and the end of financial year (end June). In contrast, for the majority of the 4-month winter period (May-Aug) across all years, the discrepancies in the 7-day trend are relatively small (particularly across Qld).

It therefore seems likely that much of the error shown in this weekly comparison (and potentially the correlation outliers shown in Figure 2) result from limitations to the comparative approach used here, rather than from flaws in this study's underlying wind modelling methodology. More specifically, the comparison provided here does not adjust for one part of AEMO's methodology, that shifts calendar days on public holidays when developing their wind, solar and demand traces.

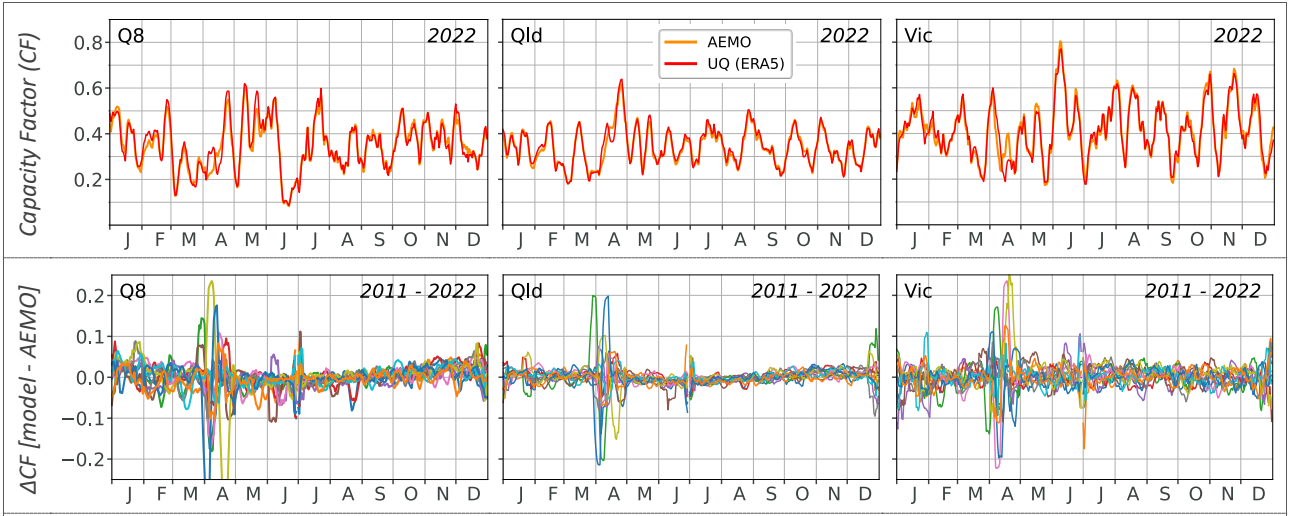

Figure 5: Weekly time-series of wind CF, comparing modelled vs AEMO results.

Trends are a rolling 7d-average of the CF data, for (a) an example time-series for the 2022 calendar year; and (b) the difference between the modelled and AEMO results, overlaying all years (each year a different colour).

The modelled solar CF match the AEMO data well, though with gaps during critical periods

Across the full comparison dataset, the weekly fit of the solar PV results (Figure 6) appears to be of similar quality to that for wind (Figure 2). However, this masks some important seasonal shortcomings with the modelled solar CF results.

The comparison of CF distributions (Figure 7) shows clearly the insufficient variance in the modelled results – for the summer and winter periods, both reanalysis products overestimate CF on days with low solar availability, and underestimate CF on days of relatively high PV output. As also indicated in Table 3, the BARRA-R2 model performs notably worse in this regard. The summer-winter and Queensland-

Victoria comparisons also show that these discrepancies are greater at times and locations of higher PV output - see also the additional scatter plot comparisons provided in Appendix B.

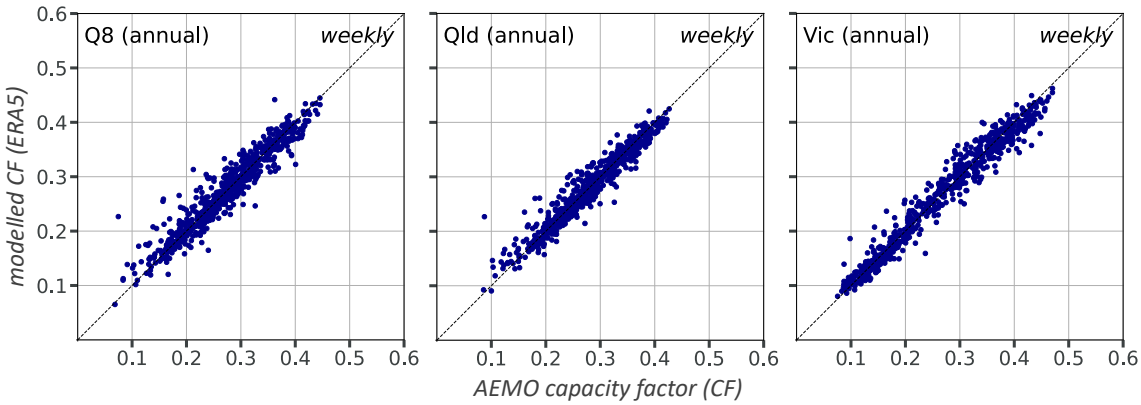

Figure 6: Comparison of modelled results vs AEMO CF over 2011-23, for weekly-avg solar CF.

Two methodological limitations likely contribute to why the statistical fit for solar PV results is not as good as for the wind modelling. Firstly, AEMO doesn't use reanalysis data in the solar PV modelling method, increasing the likelihood of error caused by the choice of weather data – see Figure 18 and Figure 19 for more analysis on this topic. Secondly, the single-term error correction used for solar PV modelling (in this study) specifically targets reductions in the mean error, however does not directly adjust for discrepancies in the variance.

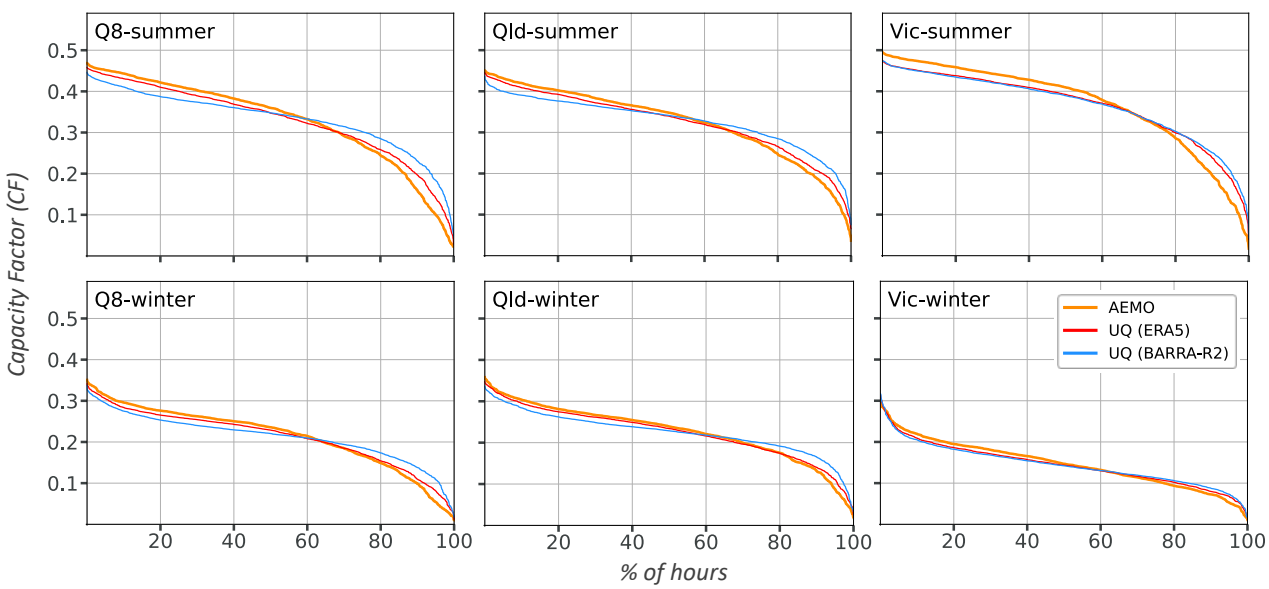

Figure 7: Generation-duration curves for daily solar CF (2011-2023), comparing both reanalysis models with AEMO.

Despite those limitations, Figure 8 confirms that the use of weekly correction factors ensures the modelled results can effectively match the variations in AEMO's CF spread across seasons, and across the very different solar resource profiles of northern and southern Australia.

Comparing the trends of 7-day solar CF (Figure 9a) illustrates the implications of the poor fit to the solar CF distribution shape. The reanalysis-modelled CF mostly follow the general trend well, though there are many periods where they mis-represent the extent of peaks or troughs in the AEMO-CF traces. Looking across all the years (Figure 9b), the positive and negative discrepancies are most notable across summer months. As with the modelled wind CF, the same concentration of comparison-error is also apparent for periods of the year that involve public holidays.

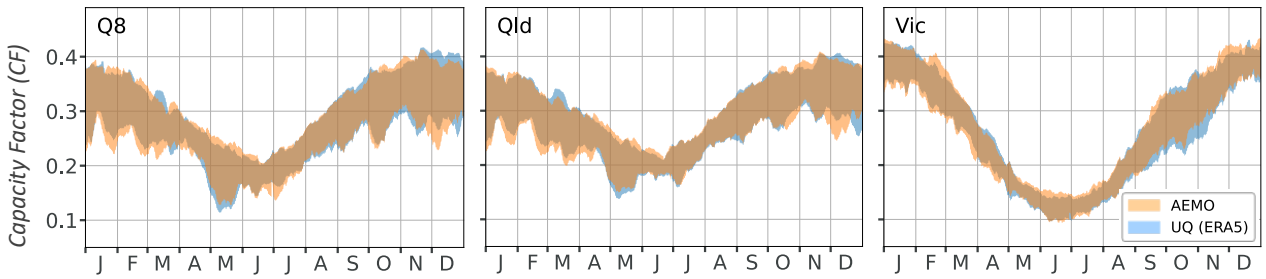

Figure 8: Seasonal spread of the solar-CF across 2011-2022, comparing modelled vs AEMO results.

For each time-series (modelled; AEMO) a 30d rolling-avg is applied; then for each calendar day, the min/max CF from any year is obtained.

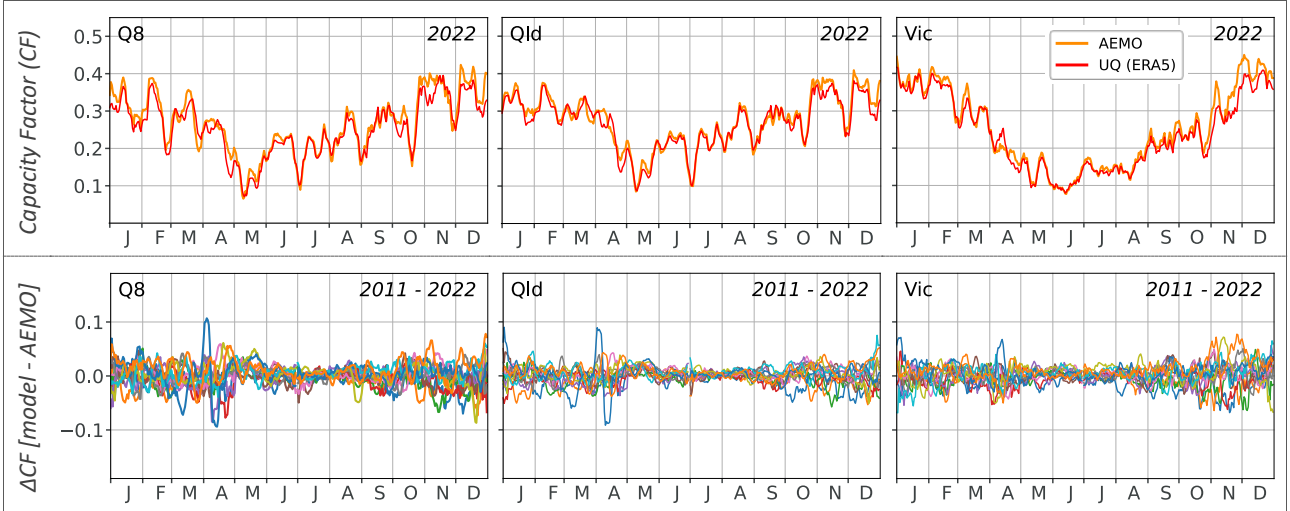

Figure 9: Weekly time-series of solar CF, comparing modelled vs AEMO results.

Trends are a rolling 7d-average of the CF data, for (a) an example time-series for the 2022 calendar year; and (b) the difference between modelled and AEMO results, overlaying all years (each year a different colour).

3.2 AEMO's 'weather years' don't capture the full range of possible variability

Reviewing the data from a range of perspectives, the analyses in this section collectively indicate that the current AEMO weather-years period (2010-11 to 2022-23) is too short to capture the potential for VRE resource variability that is apparent in a longer historical record.[q]

Figure 10 provides long-term trends of winter-averaged CF for wind and solar (lines), contrasted against the range of winter-averaged CF in the AEMO CF traces (bands), showing that the ISP *weather-years* period does not capture the lowest winter wind over the full 82yr period. In 1950 for example, the winter-average CF for Victoria and Tasmania was ~30% lower than the lowest equivalent result during the 2011-2022 winters. Winter wind in those two states drops below the AEMO range more often (and by a greater margin) than for other states, with those low years coinciding in many cases.

Comparatively, there is far less variation (over the longer historical record) in the winter-mean solar CFs, which do not demonstrably exceed the CF range captured by the AEMO reference period. The state-aggregate results also suggest that there may have been a rising trend in winter wind resources from 1940 through 1960 (and potentially up until the 1980s). It is unclear whether or not the weather patterns of that initial 20 years warrant inclusion in applied analysis of the NEM. On the one hand, the quality of reanalysis products might be lower for earlier years, given the reduced availability and quality of

[q] Since this analysis was undertaken, AEMO have announced their upcoming CF development work will add two more recent years (2023-24 and 2024-25)[31], though it is not anticipated they will extend them further back in time.

observational records in those periods. On the other hand, there exists at least one study demonstrating that the 82-year wind speed trends in ERA5 are consistent with the best available understanding of multi-decadal wind cycles over the full 20th century period[43] - suggesting that the 1940-1960 period should not be dismissed without further investigation.

Figure 10: Inter-annual variation in winter-mean CF since 1940, benchmarked against the AEMO range.
Lines show modelled CF. Bands show the spread (across 2011-2022) of winter-mean values taken from the AEMO CF traces. Solar CF for Tasmanian winter are not shown, as they fall outside the plot range used here.

Low winter-average wind is not the only important risk factor in terms of VRE resource shortfalls - more extreme (but shorter duration) drops in CF also pose a challenge to NEM supply-demand resilience.[13,44] Figure 11 assesses more extreme lows in 7-day wind CF over the 4-month winter period (May – Aug), as one possible way of assessing whether AEMO's CF data adequately captures the risk of low-probability, week-long droughts in wind supply. Other thresholds for probability and/or duration (shorter/longer than 7d) might also be considered, depending on the risks (to NEM resilience) in question.

From the annual trend of those winter-p10 values, across the NEM there are many earlier years with 7-day winter wind shortfalls lower than in the ISP weather year CF traces. As with the analysis of winter-mean CF trends above, Figure 11 also illustrates that it is the high-wind southern states (Vic, SA, Tas) that pose the greatest challenge in terms of wind volatility. Contrasting this with the state-specific results in Appendix B, it's apparent that many of the lowest wind CF weeks occur within the same year across multiple states. That suggests there may not be sufficient diversity of wind patterns (across southern Australia) to hedge against the risk of extreme winter wind lulls.

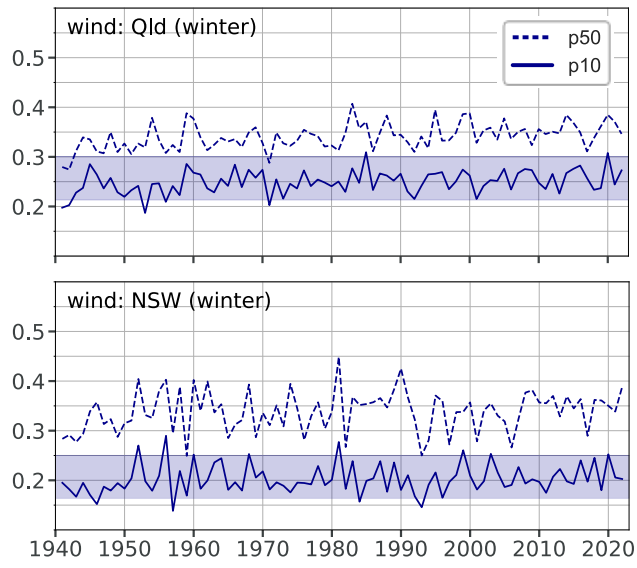

Figure 11: Inter-annual variation in quantiles of wind CF for winter, benchmarked against the AEMO range.

Median & 10th percentile of weekly avg CF (winter months), are calculated from a 7d-rolling average of CF aggregated across REZ & wind categories.

Bands show the spread (across 2011-2022) of equivalent winter p10 values for the AEMO CF traces.

When the overall NEM-wide renewables resource is considered using the same analytical approach (Figure 12), it again illustrates that **the AEMO *weather years* are insufficient to capture the low-side risk of more extreme renewable resource lulls**. Integrating across wind and PV does soften the overall extent of inter-annual variability, however there are clearly older decades where the p10 weekly VRE resource potentials were lower (and the extreme lows more common) than has occurred since 2010.

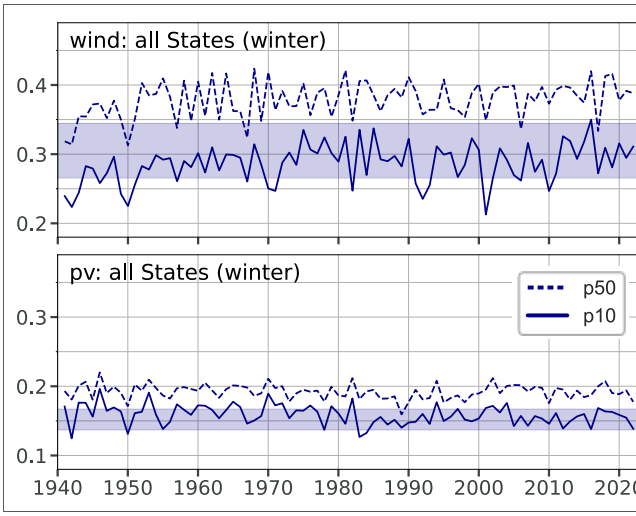

Figure 12: Inter-annual variation in quantiles of NEM-wide modelled CF (wind & solar), for winter.

Median & 10th percentile (for winter months) are calculated from a 7d-rolling average of CF.

Bands show the spread (across 2011-2022) of equivalent winter p10 values for the AEMO CF.

For a more granular perspective on seasonal diversity across the reanalysis timespans, Figure 13 adopts the same analytical approach as Figure 4 and Figure 8, but this time comparing across decades within the 80+ year historical record provided by ERA5. It shows that, for both the wind and solar resources, the intra-decadal spread in 30d-average CF increases if longer time periods are considered. These plots are layered with the oldest period on the bottom of the stack – hence they illustrate the additional spread that would be created if the set of *weather-years* is progressively extended backwards in time.

It's notable that **no single 20yr period captures the lowest 30d-avg CF profile** across the whole year, suggesting there will always be some risk in relying on an arbitrarily short set of weather years for NEM

analysis. From Appendix B, it's also apparent that there is considerable variation across seasons and across the states, in terms of which decade has the lowest 30d-avg CF performance. Furthermore, the downside risk is not just an issue for wind resources, as all states (but particularly Queensland) show decades with lower summer solar resource output than in the AEMO *weather year* period. Though when the wind and PV resources are combined to assess the overall VRE capacity for the NEM (bottom right panel of Figure 13), it is the winter months where AEMO's limited set of *weather years* are least adequate at capturing the potential for 30d periods of low VRE output.

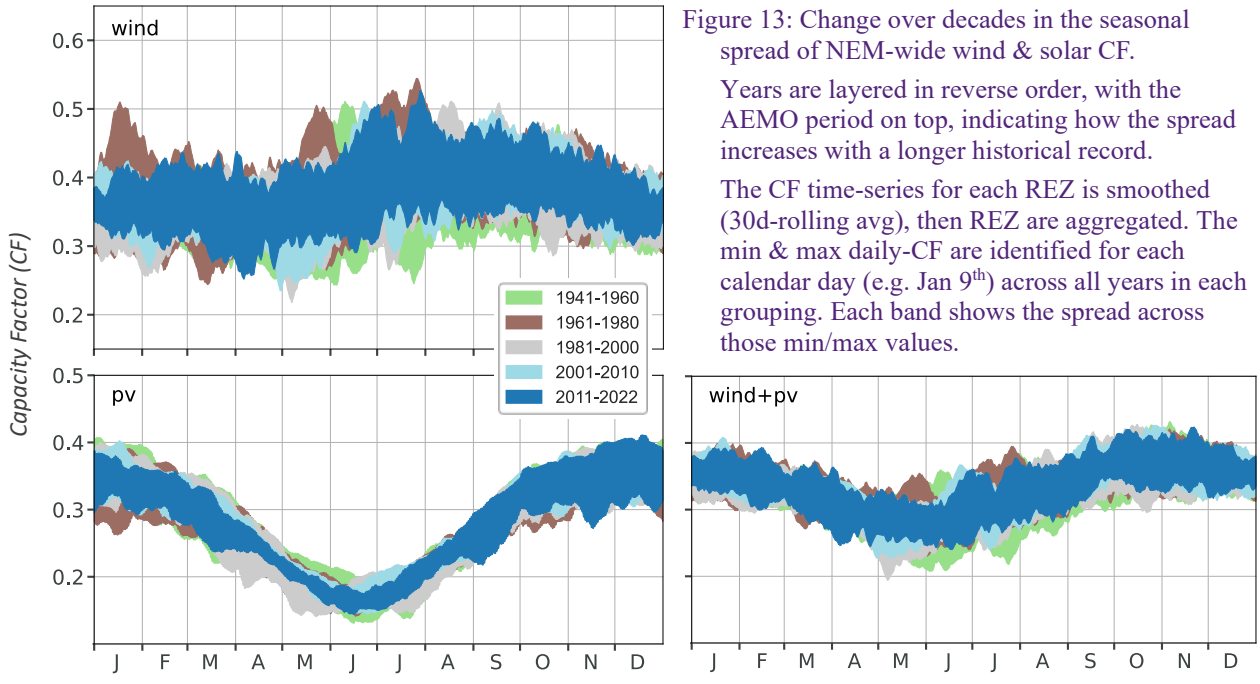

Figure 13: Change over decades in the seasonal spread of NEM-wide wind & solar CF.

Years are layered in reverse order, with the AEMO period on top, indicating how the spread increases with a longer historical record.

The CF time-series for each REZ is smoothed (30d-rolling avg), then REZ are aggregated. The min & max daily-CF are identified for each calendar day (e.g. Jan 9th) across all years in each grouping. Each band shows the spread across those min/max values.

3.3 The choice of CF data should be tailored to the risk under consideration

The above analysis indicates that neither of the two reanalysis-based CF products can be uniformly judged as the 'best' for modelling CF over long-term horizons. Furthermore, the available evidence suggests it might be equally unhelpful to ascertain that a particular historical timeframe is the best to use as the basis for modelling the sensitivity of energy transitions to uncertain future weather variability.

Instead, a more broadly useful approach would be to develop and maintain a robust set of CF alternatives, from which bespoke selections can be made as required to best suit the study in question.

Spatio-temporal relationships across weather variables are an important consideration

A crucial consideration when considering whether and how to use reanalysis-based CF profiles, is the importance (or otherwise) of maintaining key spatio-temporal relationships across the multiple weather variables that influence electricity supply (wind and solar resources) and demand (temperature). AEMO's methodologies for the ISP put a high priority on this objective, limiting their trace span to more recent years for which higher quality empirical data is available.

Maintaining consistency with this objective poses a challenge when searching for longer datasets to be used for assessing the implications of uncertain VRE resource variability. The risk in independently selecting different data sources for each of wind, solar and temperature is that important spatio-temporal relationships across the three might get lost.

Reanalysis weather data are produced using established climatological models and techniques, thereby providing some degree of internal consistency across the weather variables of interest.[35,45] Hence there is some appeal in using a single reanalysis product as the source of CF profiles across both wind and solar, and across all locations.

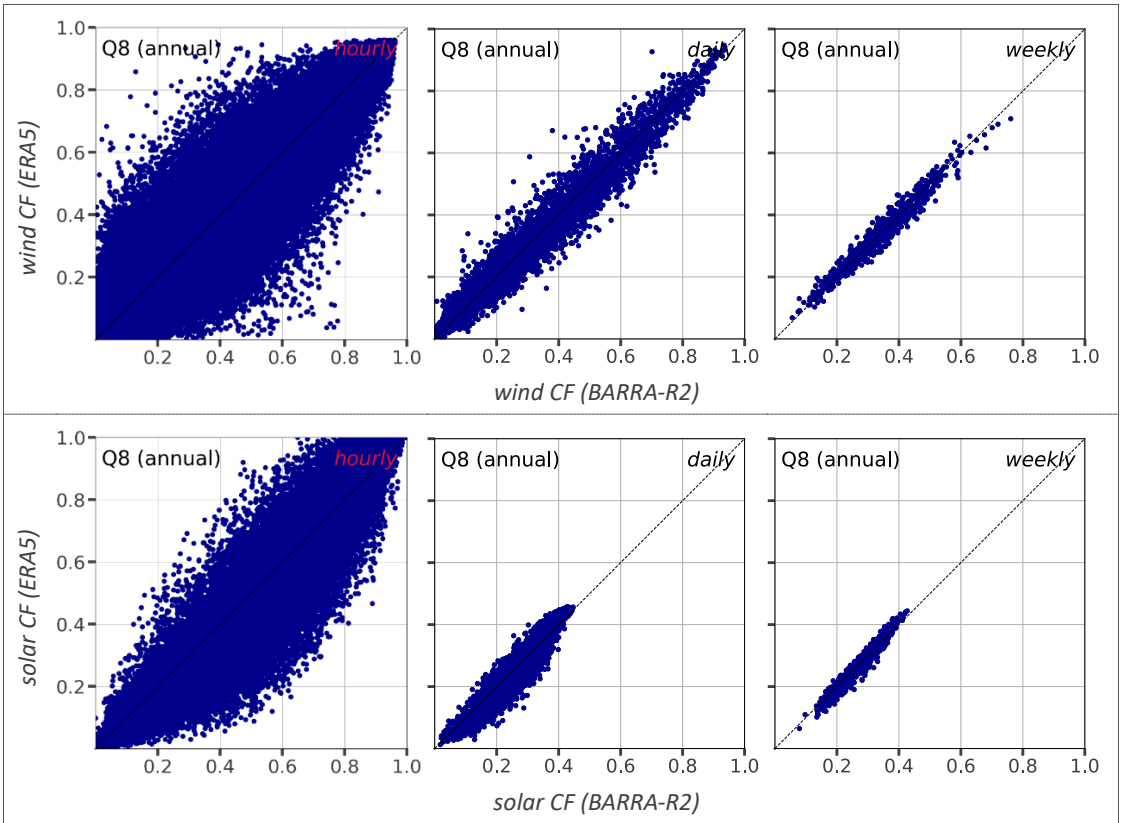

Figure 14: Comparison of the modelled CF (ERA5 vs. BARRA-R2) at different temporal resolutions. Results shown for hourly modelled CF (left), daily-avg CF (middle) and weekly-avg CF (right).

The alternative – to mix different reanalysis products across different technologies and/or regions, could potentially result in spatio-temporal combinations of wind/solar output that are not statistically representative of historical weather patterns. Figure 14 highlights that this could be a particular problem if the different REZ-level CF products were mixed for analysis with a priority on fidelity at the hourly resolution, given the hourly-scale comparison shows a wide scatter. This may be less of a concern for analysis focussed on longer timeframes, as the correlation across BARRA-R2 and ERA5 products improves dramatically for the daily and weekly-averaged CF (Figure 14; Table 4).

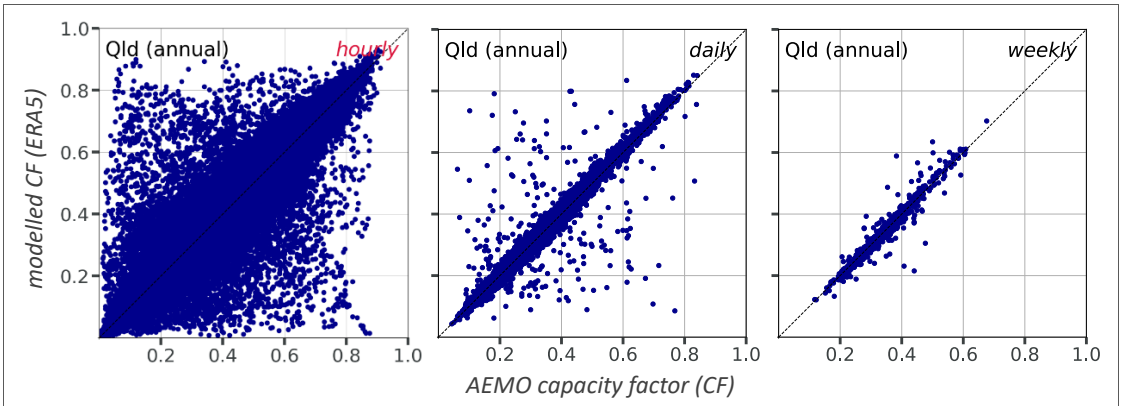

Figure 15: Comparison of the Wind CF (modelled vs. AEMO) at different temporal resolutions. Results shown for hourly modelled CF (left), daily-avg CF (middle) and weekly-avg CF (right).

Furthermore, if a longer timeseries of CF data is to be incorporated into electricity systems supply-demand modelling, it will be important to consider whether (and how) to maintain spatio-temporal relationships across renewables supply and temperature (given its strong influence on demand volatility. Figure 15 illustrates the weak hourly-scale correlation with AEMO's CF traces, suggesting some potential downsides to using the reanalysis modelled CF in combination with AEMO's demand

traces[r], even if the data is drawn from the same *'weather-year'*. Improvements to the comparison method (see Section 3.1) should reduce some of the visible scatter in Figure 15, though limitations with reanalysis data quality would likely remain a contributor to weaker correlation at the hourly-scale.

The two reanalysis-based CF products align well, but have some critical differences

When considering longer-duration analytics, the BARRA-R2 and ERA5 based products match each other well. Table 4 shows the two are well correlated even before the correction steps are applied, with that correction step delivering only a minor improvement. This suggests that the strong correlation is an intrinsic property of the two reanalysis products, rather than an artefact of the modelling and calibration methodologies used here.

Table 4: Correlation of the state-level CF (wind & solar) across the BARRA- and ERA-derived CF time series. Correlations are measured for different temporal averages (hourly, daily, weekly, monthly), repeated for the *Raw* and *Corrected* CF. State aggregates are capacity-weighted across REZ and across wind categories.

	Timestep	uncorrected CF					corrected CF				
		Qld	NSW	Vic	SA	Tas	Qld	NSW	Vic	SA	Tas
wind	hour	0.94	0.95	0.96	0.94	0.93	0.95	0.96	0.96	0.95	0.93
	day	0.97	0.98	0.98	0.97	0.96	0.98	0.98	0.98	0.98	0.96
	week	0.97	0.98	0.99	0.97	0.98	0.98	0.98	0.99	0.98	0.98
	month	0.96	0.97	0.99	0.96	0.98	0.97	0.98	0.99	0.97	0.98
solar	day	0.95	0.97	0.97	0.97	0.95	0.95	0.97	0.97	0.96	0.95
	week	0.96	0.99	0.99	0.99	0.99	0.97	0.99	0.99	0.99	0.99
	month	0.97	0.99	1.00	1.00	0.99	0.98	1.00	0.99	0.99	1.00

This is also illustrated graphically in Figure 16, showing a strong correlation of long-term trends at the seasonal level. The error correction step eliminates the mean bias across the two uncorrected CF series; resulting in the two corrected CF series having very similar cross-seasonal spreads (Figure 17).

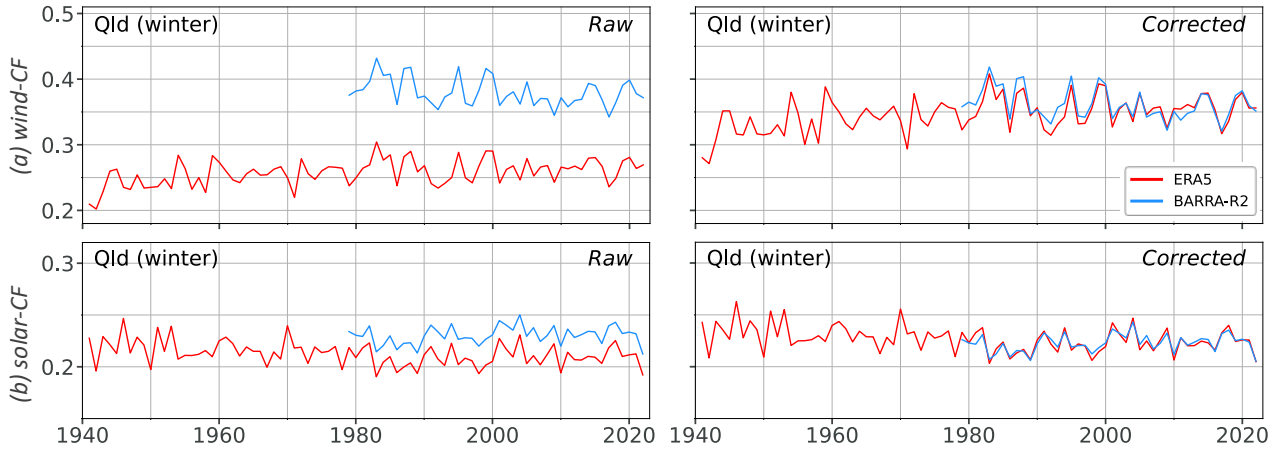

Figure 16: The effects of the error correction process, on winter-mean CF for (a) wind and (b) solar. Mean CF are shown for the raw (left) and corrected (right) model results.

Wind

As outlined in Section 3.1, the final products based on ERA5 and BARRA-R2 are very similar, with neither being universally the best fit (to the AEMO wind CF) across all wind speed ranges and across all REZ.

Note that superior performance in the comparative analyses presented here, does not convey that either product is more 'accurate' at representing real-world wind or wind-energy patterns – only that it

[r] Given AEMO puts a priority on maintaining historical spatio-temporal relationships between their CF traces and the temperature effects on electricity demand

is more representative of AEMO's CF traces. In the absence of detailed wind-farm operational data (hub height wind measurements; power output), estimating real-world 'accuracy' of the reanalysis derived CF series is problematic.[s]

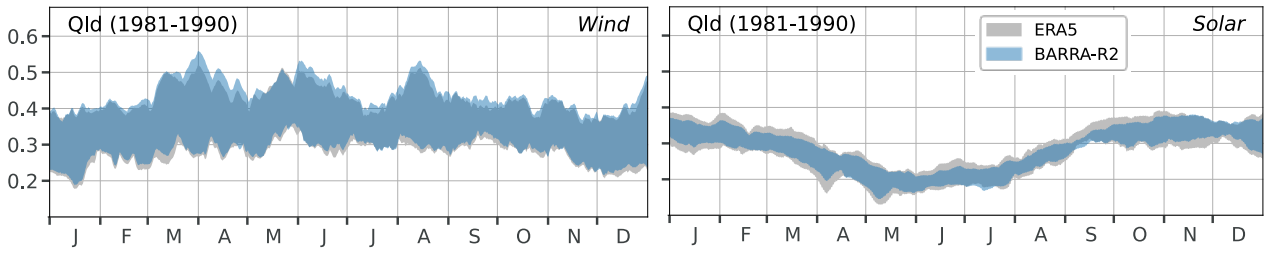

Figure 17: Comparing the seasonal spread of state-level CF (wind; solar) across the ERA5 and BARRA-R2 products. The example provided here is for Qld over the 1981-1990 decade.

Given ERA5 tends to provide a better fit to the AEMO CF traces in many locations, two perspectives are noteworthy. Firstly, other studies[16,25] and unpublished UQ analysis show that BARRA-R2 is in general the more accurate at matching observed ground-level (10m) wind speed data. This is particularly the case for the mid-speed range (5-20m/s) relevant to wind power modelling, though noting that both reanalysis products tend to underestimate ground-level wind speed during lower wind conditions. Secondly, a comparison for select wind farms in Australia concluded that CF derived from BARRA-R2 gave a better match to wind-farm performance data, than if using global reanalysis products. Perhaps for these reasons, AEMO have announced that their CF development will in future adopt BARRA-R2 as the source of reanalysis data, where they previously used ERA5[31].

Solar PV

Unlike for wind, weaknesses in matching AEMO's solar CF traces might reasonably be viewed as a limitation on the quality of solar PV assessments provided by the reanalysis-modelled CF. This is because the AEMO methodology employs a satellite-based irradiance dataset (coupled with specific plant operational data) that is likely superior in quality to the reanalysis irradiance data.

As indicated in Section 3.1, both sets of modelled CF underestimate the variance that is apparent in AEMO's CF traces, with that mismatch being more substantial for the CF produced from BARRA-R2. The modelled CF products are therefore prone to overestimating solar resource potential on summer and winter days with low irradiance conditions.

The analysis presented in Figure 18 and Figure 19 suggests that the source of this error is predominantly the reanalysis data rather than the PV power model configuration, with the error correction process then exaggerating the disparities for BARRA-R2 in particular.

Figure 18(a) shows that both the modelled CF products follow the shape of mean trends across both critical seasons, though before the error correction step is applied, BARRA-R2 produces CF that are much closer to the AEMO CF's mean. Notably, the seasonal standard deviation of both modelled CF products is notably lower than for the AEMO CF traces. For the ERA5 product, this is partially rectified through the error correction process. Whereas for BARRA-R2, because the uncorrected results match the mean so well, the error correction process makes little difference to the variance (sometimes reducing it), hence exacerbates the disparity in variance across the two sets of modelled results.

Figure 18(b) suggests that the differences in the modelled CF are explained by differences in the GHI data within each reanalysis product – the BARRA-R2 dataset shows a notably higher mean but lower standard deviation. Initial (unpublished) analysis suggests that the reanalysis cloud cover estimates

[s] Estimating 'accuracy' of the reanalysis-derived CF is difficult given a lack of quality empirical data. Publicly available VRE generation data does not provide a pure 'resource availability' perspective. Publicly available empirical wind speed data is measured at 10m, not at hub-heights. The relationship between ground & hub height wind speeds can vary strongly over time and locations; and ground observations can be a poor proxy for inter-annual trends in wind energy potential.[46]

could be an important contributor to this GHI discrepancy between the products, and the primary reason why both sets of modelled CF underestimate the variance in the AEMO benchmark. As illustrated in Figure 19, both reanalysis products (but particularly BARRA-R2) underestimate local on-the-ground cloud conditions across the whole year.

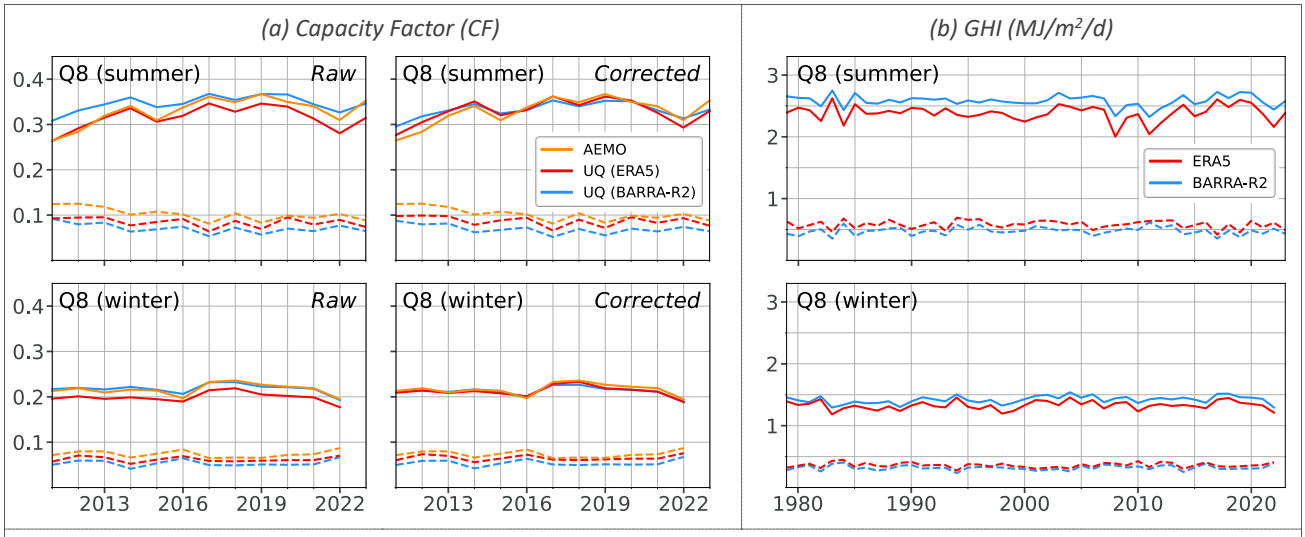

Figure 18: Comparison (ERA5 vs BARRA-R2) of inter-annual variation in solar CF & irradiance.
Seasonal mean (solid) and standard deviation (dashed) are shown for (a) the modelled and AEMO CF; and (b) reanalysis data for Global Horizontal Irradiance (GHI).

Figure 19: Seasonal error in the reanalysis model estimates of cloud cover.
For each BoM weather station within a Qld REZ boundary, monthly avg bias (= reanalysis – BoM) is calculated, then seasonal trends are averaged across all locations.

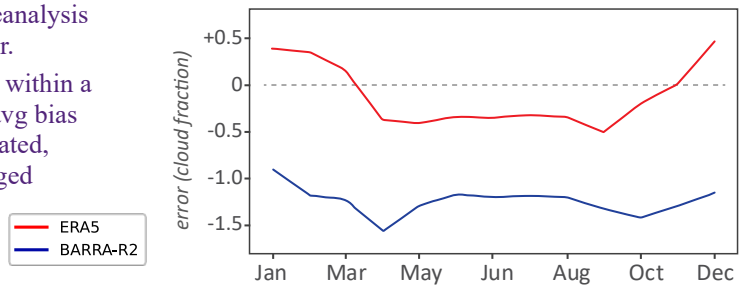

Although the CF from ERA5 might be superior at matching the longer term trends in the AEMO solar CF, the CF derived from BARRA-R2 mostly provide a better fit to the diurnal profile in AEMO's data (Figure 20). The differences in diurnal shape are most stark for the summer months in Queensland and (to a lesser extent) NSW. For the more southern REZ, the post-correction differences (across the two reanalysis products) in mean diurnal profile are negligible across the year.

Notably, the modelled CF from BARRA-R2 often has a superior fit during the critical afternoon shoulder period, when electricity demand can peak dramatically. During those periods, which remains a critical concern for near-term electricity system operations, the averaged CF profile from ERA5 can underestimate the solar resource potential.

If these CF are to be used in uncertainty analysis, then the preferred choice may depend on the particular risk that is being assessed. For wind-specific analysis, for example, the choice of using CF from BARRA-R2 or ERA5 might depend on which location and/or which season is considered most important for the risk under consideration – the ERA5 product is generally a better fit to AEMO's CF traces, however the BARRA-R2 product is sometimes better at matching the AEMO CF profile under low wind conditions in southern states (see also Figure 3 and associated commentary).

The case study presented in Section 4, provides an example where one particular CF product is deemed the most useful. That illustrates the value in having a variety of options to consider, beyond relying solely on AEMO's published CF traces.

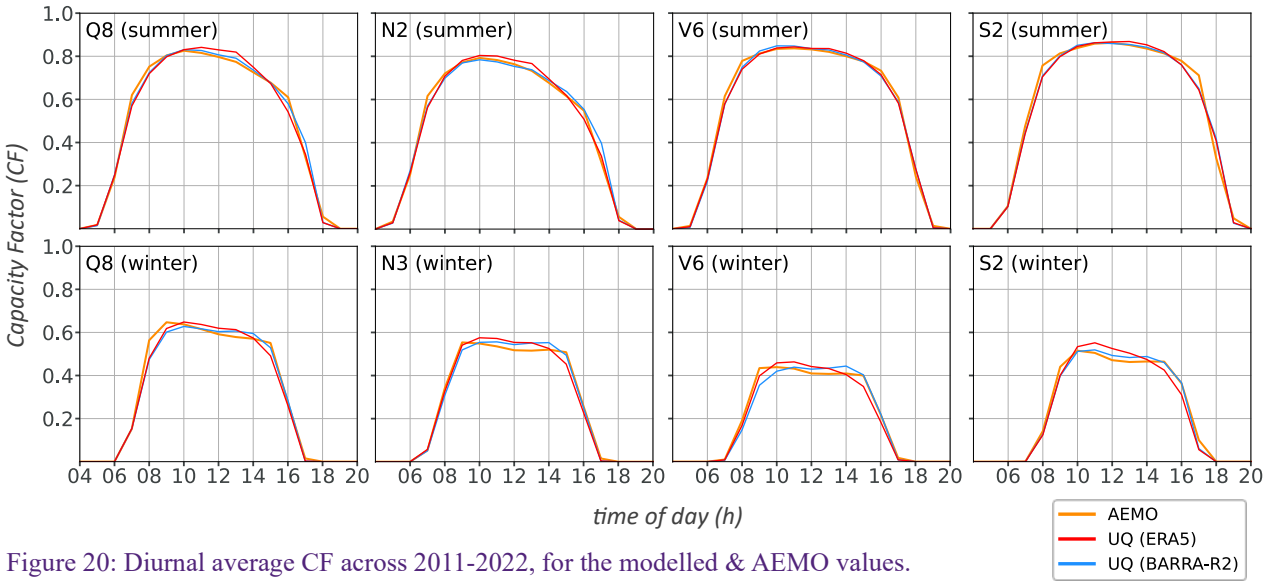

Figure 20: Diurnal average CF across 2011-2022, for the modelled & AEMO values.

Comparisons are shown for *Summer* (top) and *Winter* (bottom) months. Example REZ are shown for Qld (Q8), NSW (N2), Victoria (V6) and South Australia (S2). All times shown on the x-axis are AEST.

3.4 Methodology improvements will increase the utility of CF back-casts

Multiple opportunities for further methodological modification have been identified, each aiming to improve either the underlying CF modelling methodology, and/or extend the scope to improve how the CF can be used in subsequent uncertainty analyses.

A selection of those opportunities are grouped here into four typologies.

Reduce disparities between the modelled CF and the AEMO benchmark

The following improvements are underway at UQ, aiming to address the priority weaknesses of the CF products from this study.

For the wind modelling, three steps are being explored to reduce disparities created by the power model configuration. The first is a more individualised selection of hub-height and power-curve assumptions for each REZ, including the possibility (where relevant) of blending CF timeseries for existing and hypothetical wind farms. The second is to calibrate the simplified windpowerlib functions for wake losses and farm-level power curve smoothing, using available wind farm performance data.

For the wind modelling error correction step, incorporating an allowance for diurnal and seasonal effects is expected to yield improvements. Figure 21 illustrates the findings from other unpublished UQ analysis showing the spatially heterogeneous error between reanalysis and BoM observed data in Queensland REZ regions. BoM analysis shows similar findings in a critique across all Australian weather stations.[16] Analysis in other jurisdictions has demonstrated the importance of compensating for diurnal heterogeneities when modelling CF from reanalysis data.[47]

For the solar power modelling, more systematic consideration of methodology alternatives (e.g. panel configuration; irradiance interpolation) is being explored, aiming to improve the fit to the diurnal profile of AEMO's CF data. An alternative approach to the error correction step is also being trialled, using a heuristic that adjusts for both mean and variance, modifying the underlying weather data rather than direct manipulation of the CF results. The latter is predicated on the expectation that reanalysis cloud cover estimates are the primary source of error, as indicated in this study (see Section 3.3, Figure 19) and other analysis[20].

Tools to improve the application of long-record CF into energy system modelling

Two approaches are being trialled, aiming to finalise a screening methodology suitable for guiding users on the selection of various weather scenarios (i.e. combinations of different *weather-years*). The

motivation for this step is that most high-profile energy systems optimisation models are computationally constrained and therefore not suited for stochastic implementation. Firstly, through direct statistical characterisation of the CF time-series across the full 40 or 80 years. Second, through stochastic implementation of a simplified (deterministic) dispatch model[t], then using the distribution of results to inform the sampling of a small subset of *weather-year* combinations.

Further tool development is being explored to facilitate direct implementation of the CF back-casts into energy systems scenario modelling, aiming to provide users with the option of maintaining the spatio-temporal relationships across weather variables that influence variability in renewable supply (wind/solar) and demand (temperature).

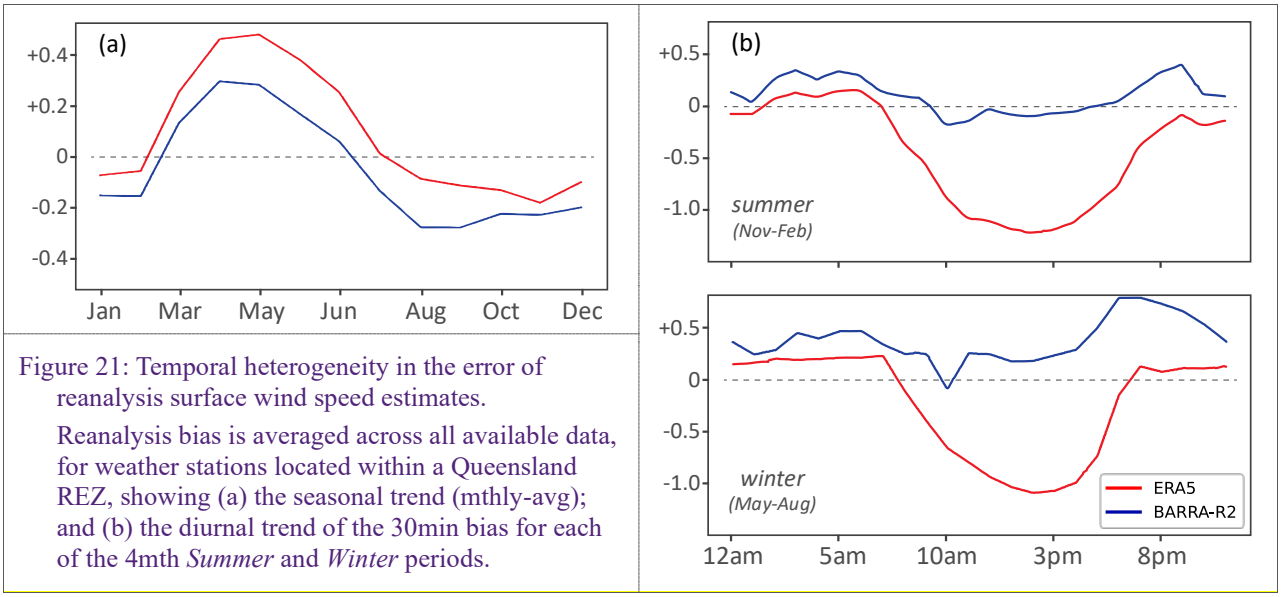

Figure 21: Temporal heterogeneity in the error of reanalysis surface wind speed estimates.

Reanalysis bias is averaged across all available data, for weather stations located within a Queensland REZ, showing (a) the seasonal trend (mthly-avg); and (b) the diurnal trend of the 30min bias for each of the 4mth *Summer* and *Winter* periods.

More systematic consideration of underlying weather uncertainty

Improved focus on the underlying weather uncertainty, would also improve the robustness of CF application into applied energy systems uncertainty analysis. Three alternatives warrant consideration.

Firstly, an informed climatological critique is needed on the very low wind resource in the first 2-3 decades of the ERA5 reanalysis product. The goal should be to ascertain whether that is (a) an expected outcome within multi-decadal climate cycles that could potentially be repeated in the future[43]; or (b) an artefact of diminished reanalysis 'quality' due to reduced availability of empirical data (used to tune the reanalysis climate models) in those older years.

Second, the recently released BARRA-C2 reanalysis product provides a higher resolution alternative to BARRA-R2, that more effectively incorporates convective effects in the underlying climate models. Further investigation could assess whether that improves the characterisation of wind heterogeneity and/or cloud cover.

Third, the BoM has also released an ensemble version of their historical reanalysis data, and it may be appropriate to directly apply the CF modelling methodology (as developed for this study) to that alternate dataset. An ensemble of CF (historical) scenarios could be a useful complement to the single deterministic representation provided by BARRA-R2, potentially providing a more robust means for estimating the probability of various VRE outcomes occurring.[u]

[t] As an example, see the simplified dispatch model described in Boston *et al.* (2022)[13]

[u] Forward-looking climate change models also provide a source of ensemble products, though further investigation would be required to ascertain (a) how best to translate this CF modelling methodology to that context, and (b) whether that would actually provide greater confidence (in the representation of future VRE variability) than could be achieved using an ensemble of historical weather trajectories.

Broaden scope of weather variability under consideration

Priority targets for scope extension would be to develop methodologies that provide an equivalent characterisation of weather-based resource uncertainty for rooftop PV and hydro generation. Neither are expected to be as significant a source of uncertainty (for applied energy system modelling) as the wind variability highlighted in this study, however the analysis here also indicates the marginal risk if other VRE shortfalls occur coincidentally with periods of low wind. Others have developed a set of state-based CF traces for rooftop PV[14], with an alternative methodology under development at UQ that aims to replicate the level of transparency and flexibility (for future improvement) that motivated the work in this study.

4. Case Study

As the NEM becomes more reliant on VRE generation, AEMO[48], state government[49] and independent[44] planning studies make it clear that the role of gas-powered electricity generation (GPG) as the *'option-of-last-resort' (OOLR)* will become more critical in the future. The *OOLR* planning challenge is a pertinent consideration here, as the uncertainties involved in estimating *OOLR* scale will be influenced by the many and compounding uncertainties across all aspects of planning an energy system transition years to decades in advance.

Enabling sufficient future GPG supply (of electricity) therefore becomes critical to maintaining NEM resilience over the long-term. GPG has traditionally been viewed as a safe-backstop to balancing electricity system supply and demand, being more reliable and/or responsive than alternative dispatchable sources. New electrical storage technologies will increasingly assume some of that role as the transition progresses. However, even under the ISP's ambitious scenarios for batteries and pumped hydro deployment, the available modelling indicates that large-scale GPG would still be required to fill weather-driven VRE supply gaps that exceed the capabilities of those technologies.

Should future GPG not be able to meet the role ascribed to it in the ISP, the risk could be material for all *electricity sector stakeholders* affected by NEM supply (un)reliability. However, the greatest planning challenge to mitigate that risk arguably falls on the *gas sector*.

The planning challenge for gas supply to GPG

AEMO's GSOO report shows that (a) the peak rates of gas supply required to service GPG operations would need to grow substantially over the next decades; and that (b) meeting those peak demands for gas could prove challenging from 2028 onwards.[41] Ensuring adequate supply to GPG in southern states (NSW, Vic, SA, Tas) will become increasingly difficult, given their reliance on the rapidly declining Victorian gas supplies, and network constraints that limit the rate of gas transfers from Queensland to the south. As Victorian gas producers have historically played a major role in meeting volatile demand swings[41,50], considerable new infrastructure will be needed to ensure the gas supply system can not only replace that lost capacity, but also meet an increasing scale of peak GPG demands.

System-wide planning to address that gas supply capability gap will be complex, made more difficult by the lack of any comprehensive and transparent options analysis in the public domain. AEMO makes clear that no one solution is likely to be sufficient, and that current infrastructure proposals could delay the risk of severe shortages by a small number of years, with the more substantial longer-term problem remaining.[41,51] Furthermore, the growing influence of GPG in determining peak gas demand requirements, introduces a spatial uncertainty that might not have been a priority gas sector concern in the past. With most other major elements of the NEM transition being highly contested, and/or suffering substantial delays and cost blowouts[52,53], there remains considerable doubt over where and when the deployment of new GPG facilities would need to proceed.

Given the uncertainties involved in future weather variability, and the complexity of the gas system planning challenge, it is useful to consider whether (or not) AEMO's estimates of GPG demand provide adequate guidance. To justify the large capital investments required, stakeholders will need quality assessments of how big, how sustained, how frequent, where and how predictable will be the future demands for gas. This study's modelled CF data are used to critique whether stakeholders should be confident that AEMO's GSOO assessment adequately covers the potential scale of gas supply system investment that would be needed to ensure long-term GPG reliability.

Assessing whether AEMO's weather-years provide robust guidance

This exploratory analysis is premised on three simplifying perspectives:

- First, it is assumed that the GSOO estimates for future peak daily gas supply requirements (see Table 5) were modelled using wind and solar CF traces developed by AEMO for the ISP-2024, hence only considered weather patterns from the years 2010-11 to 2022-23.

AEMO specifies that 10 different weather scenarios were used in the GSOO uncertainty analysis, but doesn't provide further details on what those scenarios entail. Given AEMO does state that the GSOO forecasts for GPG align with both the methodology and results of the ISP-2024[41,54], this analysis assumes that the GSOO's weather scenarios are a subset of the CF scenarios developed for the ISP. Each of those ISP weather scenarios provides a multi-year projection comprising different combinations of the CF traces from AEMO's 13 *weather-years* (2010-11 to 2022-23) – i.e. the same benchmark period referred to in previous sections of this report.

- Second, the focus is on the challenges created by longer-duration winter VRE shortfalls.

  AEMO and other [44,v] analysis indicate that, as the NEM's reliance on VRE increases, such winter shortfalls will become the most severe challenge for GPG planning to support the NEM. Sub-daily shortfalls are not the primary concern here, given the existing gas supply networks are able to accommodate some degree of shorter-term swings through network pressure management, and this shorter-term responsiveness may increase if GPG facilities are bolstered with their own local gas storage capabilities[w]. However, winter shortfalls of VRE (particularly wind in southern states) sustained for multiple days or weeks pose a challenge that will exceed that inherent gas network swing capacity, and the capacity of any committed infrastructure investments currently in place across the broader gas system. Critically, they will also far exceed the storage duration of future electricity system storage infrastructure (batteries, pumped hydro) envisaged by the ISP.

- Finally, to assess the potential significance of VRE shortfalls that might not be captured by AEMO's CF traces, a conservative calculation approach (aiming to err on the low side) is used to quantify the potential scale of *additional* OOLR capacity that might have been required under winter weather patterns from older years.

  This is then translated to an additional need for gas supply to GPG, assuming that: (a) with GPG operating as the *OOLR* for the future NEM, any marginal shortfall in VRE output beyond that anticipated by AEMO's planning studies, would need to be serviced by *additional* GPG output; and (b) therefore in the worst case, the greater GPG output would need *additional* gas supply over and above what is anticipated by the GSOO.

To implement the analysis, the following approach was adopted:

i. The ERA5-based CF product is used because it provides the longest possible time-series of potentially valid wind- and solar-resource patterns, and provides the better overall match to the longer-term variance (in the AEMO CF traces) across both wind and solar output.[x]

   This analysis may underestimate the risks of low overall VRE output, for two reasons: (i) The modelled CF tend for large-scale (centralised) solar tend to overestimate solar potential during low periods (as identified in Section 3)[y]; and (ii) It does not account for the possibility that AEMO also underestimates shortfalls in output from a large future fleet of small-scale (rooftop) solar PV.

ii. The calculations are based on the low-side of the (30d-smoothed) spread analysis described in Figure 13. For each future scenario year, the aggregate profiles are generated using the ISP's *Step Change* scenario capacity mix for that year - Figure 22a illustrates the overall shortfall potential using the year-2050 capacity mix.

   This first set of results is limited to the four southern states because (a) constraints on winter wind generation in those regions are likely to be the biggest source of future low-side VRE resource uncertainty; and (b) the concerns (noted above) about gas supply reliability in those same states.

[v] see also forthcoming UQ analysis

[w] The new Hunter Power Project GPG facility will have 10+hr local storage, with similar approaches being considered elsewhere.

[x] Though BARRA-R2 provides better fidelity to the AEMO data during afternoon periods critical to peak summertime challenges, sub-daily considerations aren't the primary source of longer-term risk considered here.

[y] The modelled CF also underestimate solar output in periods of high solar resource potential. However, the implications of suppressed CF variance are not likely to be symmetrical, as storage capacity limits will (at times) constrain how much solar surplus can be captured. Hence the overestimate of low-solar output is likely to be more important to this risk analysis, than the underestimate of high solar output.

iii. For each day in winter (and for each future year), the gap (delta-CF) is calculated between the lowest (smoothed) daily CF within the 13 years used by the ISP (represented by the solid black line in Figure 22a) and the lowest (smoothed) daily CFs of the ERA record (dashed black line).

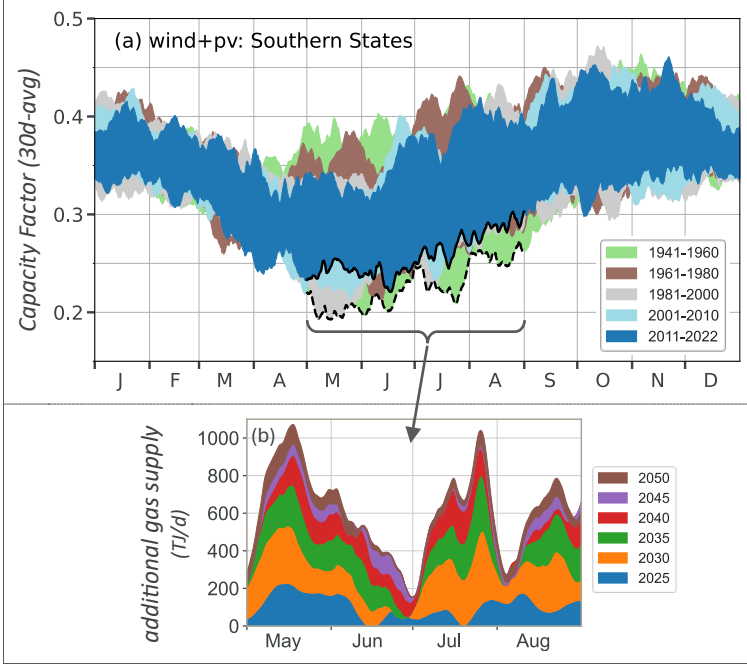

Figure 22: Derivation of the underestimate in potential gas supply requirements

(a) uses the same calculation approach as Figure 13, combining across Wind & PV for 4 states (NSW,Vic,SA,Tas).

Each year in the Step Change scenario uses a different capacity mix for the weighted avg (example shown is for 2050).

For each scenario year, the aggregate CF *underestimate* is based on the daily differences between the minimum of the AEMO period (solid black line) and the minimum across any year (dashed black line).

(b) illustrates how the need for *additional* peak daily gas supply might grow as the energy transition proceeds, if GPG is to compensate for all additional winter VRE shortfalls.

iv. For each future year in the ISP2024 Step Change scenario, the potential for (additional) VRE generation shortfall (MWh/d) is calculated by combining the aggregate delta-CF (from step iii) with the Step Change VRE (wind and solar PV) capacity for that year. This shortfall is then converted to gas supply units (TJ/d) using an average GPG heat rate of 10 GJ/MWh. Figure 22b illustrates how the scale of that (potential) *additional* gas supply grows, as VRE capacity increases over the course of the *Step Change* scenario.

v. The (potential) requirement for additional gas supply in each future scenario year is derived from those gas supply profiles (step iv), by taking the 75th percentile value from all 24h totals over the four-month winter period. This estimate is used to illustrate the potential implications of winter-averaged VRE shortfalls not captured by AEMO's 13x *weather-years*.

vi. Finally, that potential shortfall in GPG supply requirement (from step v), not captured in the AEMO weather years, is compared with the GSOO's own predictions for the maximum daily gas supply required to meet future GPG demand in the southern states (Table 5).

Table 5: Potential underestimate in AEMO's peak daily gas supply requirements for GPG - Southern states

Results (rounded to the nearest 10) aggregate across NSW, Vic, SA, Tas. The 'estimated additional gas supply required' is derived from the difference between the lowest 30d-avg CF across the winter months of 2011-2022, and the lowest 30d-avg CF across the winter months of older years – as visually illustrated in Figure 22.

Year		2030	2031	2032	2033	2034	2035	2036	2037	2038	2039	2040	2041	2042	2043	2044
GSOO peak forecast *(Step Change scenario)*	(TJ/d)	760	750	770	940	1410	1520	1440	1630	1810	1910	1890	1970	1890	1890	1990
estimated *additional* gas supply required to meet the larger VRE shortfalls in years 1940-2010	(TJ/d)	390	430	460	490	510	570	600	620	650	670	690	700	700	720	710
potential *increase* in gas supply capacity required	**(%)**	**51%**	**58%**	**60%**	**52%**	**36%**	**37%**	**41%**	**38%**	**36%**	**35%**	**36%**	**35%**	**37%**	**38%**	**36%**

Table 5 indicates that AEMO's methodology, which relies on a limited set of recent historical weather data, risks underestimating the requirements for peak daily gas supply (to southern states) by a

considerable margin. Using the longer historical weather record available in the ERA5 reanalysis product, and the simplified comparative approach adopted here, the additional (potential) gas supply requirements represent a 35-60% increase over and above the GSOO predictions across all the longer-term years of AEMO's gas supply system modelling.

To better understand this risk in the context of domestic gas production capability, Table 6 repeats the analysis for all five NEM states, with Queensland included in both the GSOO forecast and in the illustrative estimate for *unanticipated* GPG demand for gas. The increase in peak daily gas supply capacity that might be required (29-57%) is of similar proportions to that shown in Table 5. Notably, the total requirement for gas supply to GPG *[GSOO estimate + the additional estimate derived from this case study]* is ~4300TJ/d in 2044, more than four times what has ever been provided to the NEM GPG fleet historically[41].

Table 6: Potential underestimate in AEMO's peak daily gas supply requirements for GPG – all NEM states

Estimates are derived and presented as per Table 5, but including all states in the NEM (Qld, NSW, Vic, SA, Tas).

Year		2030	2031	2032	2033	2034	2035	2036	2037	2038	2039	2040	2041	2042	2043	2044
GSOO peak forecast *(Step Change scenario)*	(TJ/d)	1020	1130	1150	1340	1920	2240	2200	2420	2690	2790	2780	2940	3120	3290	3360
estimated ***additional*** gas supply required to meet the larger VRE shortfalls in years 1940-2010	(TJ/d)	570	640	660	700	750	840	880	900	920	930	940	950	950	980	980
potential *increase* in gas supply capacity required	**(%)**	**56%**	**57%**	**57%**	**52%**	**39%**	**38%**	**40%**	**37%**	**34%**	**33%**	**34%**	**32%**	**30%**	**30%**	**29%**

The estimates provided in this case study are not intended (nor sufficient) to be the basis for deterministic planning decisions. Nonetheless, they do illustrate that **by limiting their CF traces to only a small number of historical years, AEMO could potentially be underestimating the need for *OOLR* capacity by a considerable margin**. Given AEMO's planning studies all assume that GPG will provide the bulk of that *OOLR* role, and given the challenges involved in ensuring there would be sufficient gas supply capability, this uncertainty could pose a material risk to the resilience of the future NEM.

Finally, note that replacing GPG as the primary *OOLR* firming technology does not diminish the need for more systematic uncertainty analysis on future VRE supply variability. The GSOO estimates are expressed as a gas supply requirement, but in essence represent the more generic need for backup NEM supply once VRE, hydro and storage options are exhausted. GPG is routinely chosen for this role, as the scenario modelling finds it to be the cheapest and most plausible option available, *at the scale required*. But **regardless of which technology mix evolves to provide that *OOLR* service, the challenge for infrastructure planning and investment will be profound**.

Quantifying the scale of future *OOLR* service will be inherently uncertain, with planners (and the Australian community) facing a choice between (a) large-scale investment of at-risk capex, or (b) trusting that some other novel intervention will evolve (cost-effectively) as the NEM coal fleet retires. Australia's energy transition planners would be well served to undertake more systematic analysis on the scale, timing and location of future *OOLR* capacity that might be required to buffer for uncertain future VRE variability. **A forthcoming UQ report** will provide a more comprehensive analysis of the growing volatility in demand for GPG, as the NEM's transition proceeds.

Recommendations

1. **Energy transition uncertainty analysis would be improved by using CF that cover a longer set of historical years, than has been available in AEMO's published CF data.** REZ-level analysis shows multiple examples of 7-day, 30-day and 120-day periods of VRE generation potential that are considerably lower than captured by the 13 years of CF data used in AEMO's prior planning studies.

   A simplified case study illustrates the potential significance of those unanticipated shortfalls, showing that AEMO's limited set of weather-years could underestimate the burden on gas powered electricity generation (GPG) by ~30-60%. That creates considerable uncertainty for those responsible for planning capacity expansion of GPG and the associated gas supply infrastructure that would be needed, and therefore considerable risk to future NEM resilience.

   Energy system planners should prioritise more systematic analysis on the scale, timing and location of future *OOLR* capacity that might be required to buffer for uncertain future VRE variability.

2. **The REZ-level CF data produced for this report are adequate for this task, though care is needed to ensure the chosen product is fit-for-purpose to any specific analyses.** Distinct CF products were developed using the ERA5 (80yrs) and BARRA-R2 (40yrs) reanalysis data as weather inputs. Choosing between the two should be tailored to the needs of any given analysis, as their relative strengths vary spatially, temporally and by electricity system risk factor.

   These products have suppressed variance in the solar CF, making them prone to underestimating the depth of solar resource shortfalls. However that doesn't preclude their use for all purposes (such as the case study included in this report), as they provide a conservative estimate of overall risk for winter periods driven primarily by uncertain future wind variability.

3. **Multiple opportunities exist for relatively minor modifications to the methodology adopted here, which could increase the utility of the CF products.** Reducing disparities between the modelled and AEMO CF traces, would reduce some of the constraints to using this product, and likely reduce key differences between the two distinct CF products.

4. **Further tool development is warranted, to facilitate more effective use of these (and other) alternate CF products in system-level energy transition modelling.** Two priorities would be (i) Screening tools to ascertain the potential system-wide significance of different weather scenarios (i.e. different combinations of historical weather-years), to inform selective use in the more computationally intensive energy system optimisation models that underpin much of the NEM's planning analysis; and (ii) An approach to modify AEMO demand profiles, sufficient to support (screening-level) uncertainty analysis focussed on weather variability.

5. **More extensive consideration of weather uncertainty is necessary to improve the statistical robustness of CF application in uncertainty analysis, with multiple investigations worth pursuing.** Firstly, an informed climatological critique should assess whether the low wind resource in the earliest decades of the ERA5 reanalysis product, are valid for inclusion in the modelling of future energy systems. Secondly, the CF time-series development could incorporate recently published ensemble products, that may better characterise the distribution of weather possibilities.

6. **Extend the scope of this CF development to include rooftop solar PV and hydro generation.** Though neither are likely to be as substantial a source of uncertainty as wind variability, any marginal addition in *unanticipated* VRE shortfall could be significant in energy transition uncertainty analysis.

7. **Improved transparency of AEMO's CF modelling methodology would greatly improve the capacity for others to develop complementary CF datasets.** Effective uncertainty analysis requires a much broader base of research effort, which would inherently benefit from comparing and contrasting the implications of using different datasets and modelling methodologies.

References

(1) QG. *Queensland Energy and Jobs Plan - Power for Generations*; Queensland Government (QG): Brisbane, 2022. https://www.epw.qld.gov.au/energyandjobsplan/about.

(2) Davis, D.; Pascale, A.; Vecchi, A.; Bharadwaj, B.; Jones, R.; Strawhorn, T.; Tabatabaei, M.; Lopez Peralta, M.; Zhang, Y.; Beiraghi, J.; Kiri, U.; Vosshage, O.; Finch, B.; Batterham, R.; Bolt, R.; Brear, M.; Cullen, B.; Domansky, K.; Eckard, R.; Greig, C.; Keenan, R.; Smart, S. *Modelling Summary Report - Net Zero Australia*; 2023. https://www.netzeroaustralia.net.au/.

(3) AEMO. *2024 Integrated System Plan*; Australian Energy Market Operator (AEMO), 2024. https://www.aemo.com.au/energy-systems/major-publications/integrated-system-plan-isp/2024-integrated-system-plan-isp.

(4) QT. *Queensland Energy Roadmap 2025*; The State of Queensland - Queensland Treasury (QT), 2025.

(5) Bloomfield, H. C.; Brayshaw, D. J.; Shaffrey, L. C.; Coker, P. J.; Thornton, H. E. Quantifying the Increasing Sensitivity of Power Systems to Climate Variability. *Environmental Research Letters* **2016**, *11* (12). https://doi.org/10.1088/1748-9326/11/12/124025.

(6) Mallapragada, D. S.; Junge, C.; Wang, C.; Pfeifenberger, H.; Joskow, P. L.; Schmalensee, R. Electricity Pricing Challenges in Future Renewables-Dominant Power Systems. *Energy Econ.* **2023**, *126*. https://doi.org/10.1016/j.eneco.2023.106981.

(7) Simshauser, P.; Gilmore, J. Climate Change Policy Discontinuity & Australia's 2016-2021 Renewable Investment Supercycle. *Energy Policy* **2022**, *160*. https://doi.org/10.1016/j.enpol.2021.112648.

(8) Nelson, T.; Conboy, P.; Hancock, A.; Hirschhorn, P. *National Electricity Market Wholesale Market Settings Review - Draft Report*; 2025; p 239. https://www.dcceew.gov.au/energy/markets/nem-wms-review.

(9) Lee, D.; Lane, J. Managing Reserve Uncertainty in High-DER Power Systems During Peak Demand Events: An Australian Case Study; IEEE: Brisbane, 2025.

(10) Simshauser, P. Missing Money, Missing Policy and Resource Adequacy in Australia's National Electricity Market. *Util. Policy* **2019**, *60*. https://doi.org/10.1016/j.jup.2019.100936.

(11) Csereklyei, Z.; Manchester, J.; Ancev, T. Coal Generator Revenues and the Rise of Renewable Generation: Evidence from Australia's National Electricity Market. *Energy Policy* **2023**, *178*. https://doi.org/10.1016/j.enpol.2023.113580.

(12) Henckes, P.; Frank, C.; Küchler, N.; Peter, J.; Wagner, J. Uncertainty Estimation of Investment Planning Models under High Shares of Renewables Using Reanalysis Data. *Energy* **2020**, *208*. https://doi.org/10.1016/j.energy.2020.118207.

(13) Boston, A.; Bongers, G. D.; Bongers, N. Characterisation and Mitigation of Renewable Droughts in the Australian National Electricity Market. *Environmental Research Communications* **2022**, *4* (3). https://doi.org/10.1088/2515-7620/ac5677.

(14) Gilmore, J.; Nelson, T.; Nolan, T. *Quantifying the Risk of Renewable Energy Droughts in Australia's National Electricity Market (NEM) Using MERRA-2 Weather Data*; Centre for Applied Energy Economics & Policy Research: Working Paper Series 2022-23; 2022; p 28.

(15) GVSC; G-R. Appendix 26: 100% Renewables. In *Generator Insights 2021*; Global-Roam (G-R), 2021.

(16) Su, C.-H.; Rennie, S.; Torrance, J.; Dharssi, I.; Tian, S.; Howard, E.; Pepler, A.; Stassen, C.; Steinle, P. *Preliminary Assessment of Regional Moderate-Resolution Atmospheric Reanalysis for Australia*; BRR084; Bureau of Meteorology: Australia, 2023.

(17) McKenna, R.; Pfenninger, S.; Heinrichs, H.; Schmidt, J.; Staffell, I.; Bauer, C.; Gruber, K.; Hahmann, A. N.; Jansen, M.; Klingler, M.; Landwehr, N.; Larsén, X. G.; Lilliestam, J.; Pickering, B.; Robinius, M.; Tröndle, T.; Turkovska, O.; Wehrle, S.; Weinand, J. M.; Wohland, J. High-Resolution Large-Scale Onshore Wind Energy Assessments: A Review of Potential Definitions, Methodologies and Future Research Needs. *Renewable Energy* **2022**, *182*, 659–684. https://doi.org/10.1016/j.renene.2021.10.027.

(18) Gualtieri, G. Analysing the Uncertainties of Reanalysis Data Used for Wind Resource Assessment: A Critical Review. *Renewable and Sustainable Energy Reviews* **2022**, *167*, 112741. https://doi.org/10.1016/j.rser.2022.112741.

(19) Gruber, K.; Regner, P.; Wehrle, S.; Zeyringer, M.; Schmidt, J. Towards Global Validation of Wind Power Simulations: A Multi-Country Assessment of Wind Power Simulation from MERRA-2 and ERA-5 Reanalyses Bias-Corrected with the Global Wind Atlas. *Energy* **2022**, *238*, 121520. https://doi.org/10.1016/j.energy.2021.121520.

(20) Mathews, D.; Ó Gallachóir, B.; Deane, P. Systematic Bias in Reanalysis-Derived Solar Power Profiles & the Potential for Error Propagation in Long Duration Energy Storage Studies. *Applied Energy* **2023**, *336*. https://doi.org/10.1016/j.apenergy.2023.120819.

(21) Staffell, I.; Pfenninger, S. Using Bias-Corrected Reanalysis to Simulate Current and Future Wind Power Output. *Energy* **2016**, *114*, 1224–1239. https://doi.org/10.1016/j.energy.2016.08.068.

(22) Pfenninger, S.; Staffell, I. Long-Term Patterns of European PV Output Using 30 Years of Validated Hourly Reanalysis and Satellite Data. *Energy* **2016**, *114*, 1251–1265. https://doi.org/10.1016/j.energy.2016.08.060.

(23) Gunturu, U. B.; Hallgren, W. Asynchrony of Wind and Hydropower Resources in Australia. *Scientific Reports* **2017**, *7* (1). https://doi.org/10.1038/s41598-017-08981-0.

(24) Hallgren, W.; Gunturu, U. B.; Schlosser, A. The Potential Wind Power Resource in Australia: A New Perspective. *PLoS ONE* **2014**, *9* (7). https://doi.org/10.1371/journal.pone.0099608.

(25) Cowin, E.; Wang, C.; Walsh, S. D. C. Assessing Predictions of Australian Offshore Wind Energy Resources from Reanalysis Datasets. *Energies* **2023**, *16* (8). https://doi.org/10.3390/en16083404.

(26) Palmer, G.; Dargaville, R.; Su, C.-H.; Wang, C.; Hoadley, A.; Honnery, D. Validation of BARRA2 and Comparison with MERRA-2 and ERA5 Using Historical Wind Power Generation. *JSHESS* **2025**, *75* (1). https://doi.org/10.1071/ES24028.

(27) Rey-Costa, E.; Elliston, B.; Green, D.; Abramowitz, G. Firming 100% Renewable Power: Costs and Opportunities in Australia's National Electricity Market. *Renew. Energy* **2023**, *219*. https://doi.org/10.1016/j.renene.2023.119416.

(28) Li, C.; Chyong, C. K.; Reiner, D. M.; Roques, F. Taking a Portfolio Approach to Wind and Solar Deployment: The Case of the National Electricity Market in Australia. *Appl. Energy* **2024**, *369*. https://doi.org/10.1016/j.apenergy.2024.123427.

(29) Boston, A.; Bongers, G. MEGS: Modelling Energy and Grid Services to Explore Decarbonisation of Power Systems at Lowest Total System Cost. *Energy Strateg. Rev.* **2021**, *38*. https://doi.org/10.1016/j.esr.2021.100709.

(30) Su, C.-H.; Eizenberg, N.; Steinle, P.; Jakob, D.; Fox-Hughes, P.; White, C. J.; Rennie, S.; Franklin, C.; Dharssi, I.; Zhu, H. BARRA v1.0: The Bureau of Meteorology Atmospheric High-Resolution Regional Reanalysis for Australia. *Geoscientific Model Dev.* **2019**, *12* (5), 2049–2068. https://doi.org/10.5194/gmd-12-2049-2019.

(31) AEMO. *2025 Inputs, Assumptions and Scenarios Report*; Australian Energy Market Operator (AEMO), 2025. https://www.aemo.com.au/energy-systems/major-publications/integrated-system-plan-isp/2026-integrated-system-plan-isp/2025-26-inputs-assumptions-and-scenarios.

(32) Rienecker, M. M.; Suarez, M. J.; Gelaro, R.; Todling, R.; Bacmeister, J.; Liu, E.; Bosilovich, M. G.; Schubert, S. D.; Takacs, L.; Kim, G.-K.; Bloom, S.; Chen, J.; Collins, D.; Conaty, A.; Silva, A. da; Gu, W.; Joiner, J.; Koster, R. D.; Lucchesi, R.; Molod, A.; Owens, T.; Pawson, S.; Pegion, P.; Redder, C. R.; Reichle, R.; Robertson, F. R.; Ruddick, A. G.; Sienkiewicz, M.; Woollen, J. MERRA: NASA's Modern-Era Retrospective Analysis for Research and Applications. *Journal of Climate* **2011**, *24* (14), 3624–3648. https://doi.org/10.1175/JCLI-D-11-00015.1.

(33) Copernicus Climate Change Service. ERA5 Hourly Data on Single Levels from 1940 to Present, 2024. https://doi.org/0.24381/cds.adbb2d47.

(34) Hersbach, H.; Bell, B.; Berrisford, P.; Hirahara, S.; Horányi, A.; Muñoz-Sabater, J.; Nicolas, J.; Peubey, C.; Radu, R.; Schepers, D.; Simmons, A.; Soci, C.; Abdalla, S.; Abellan, X.; Balsamo, G.; Bechtold, P.; Biavati, G.; Bidlot, J.; Bonavita, M.; De Chiara, G.; Dahlgren, P.; Dee, D.; Diamantakis, M.; Dragani, R.; Flemming, J.; Forbes, R.; Fuentes, M.; Geer, A.; Haimberger, L.; Healy, S.; Hogan, R. J.; Hólm, E.; Janisková, M.; Keeley, S.; Laloyaux, P.; Lopez, P.; Lupu, C.; Radnoti, G.; de Rosnay, P.; Rozum, I.; Vamborg, F.; Villaume, S.; J-N. *Complete ERA5 from 1940: Fifth Generation of ECMWF Atmospheric Reanalyses of the Global Climate*; Copernicus Climate Change Service (C3S) Data Store (CDS), 2017. DOI: 10.24381/cds.143582cf.

(35) Su, C.-H.; Rennie, S.; Dharssi, I.; Torrance, J.; Smith, A.; Le, T.; Steinle, P.; Stassen, C.; Warren, R. A.; Wang, C.; Le Marshall, J. *BARRA2: Development of the next-Generation Australian Regional Atmospheric Reanalysis*; Bureau Research Report; 067; Australian Government Bureau of Meteorology, 2022.

(36) Haas, S.; Krien, U.; Schachler, B.; Bot, S.; Zeli, V.; Maurer, F.; Shivam, K.; Witte, F.; Rasti, S. J.; Seth; Bosch, S. Windpowerlib: Update Release, 2024. https://doi.org/10.5281/zenodo.10685057.

(37) Anderson, K. S.; Hansen, C. W.; Holmgren, W. F.; Jensen, A. R.; Mikofski, M. A.; Driesse, A. Pvlib Python: 2023 Project Update. *JOSS* **2023**, *8* (92), 5994. https://doi.org/10.21105/joss.05994.

(38) Maxwell, E. L. *A Quasi-Physical Model for Converting Hourly Global Horizontal to Direct Normal Insolation*; SERI/TR-215-3087; Solar Energy Research Inst., Golden, CO (USA), 1987. https://www.osti.gov/biblio/5987868 (accessed 2025-10-05).

(39) Perez, R.; Ineichen, P.; Seals, R.; Michalsky, J.; Stewart, R. Modeling Daylight Availability and Irradiance Components from Direct and Global Irradiance. *Sol. Energy* **1990**, *44* (5), 271–289. https://doi.org/10.1016/0038-092X(90)90055-H.

(40) Lee, D. *Keeping up with the curtailment 2024: A little? too much? or much ado about nothing?*. WattClarity. https://wattclarity.com.au/articles/2025/02/keeping-up-with-the-curtailment-2024-a-little-too-much-or-much-ado-about-nothing/ (accessed 2025-10-05).

(41) AEMO. *2025 Gas Statement of Opportunities GSOO*; Australian Energy Market Operator (AEMO), 2025. https://aemo.com.au/energy-systems/gas/gas-forecasting-and-planning/gas-statement-of-opportunities-gsoo.

(42) AEMO. *NEM Market Suspension and Operational Challenges in June 2022*; Australian Energy Market Operator (AEMO), 2022. https://www.aemo.com.au/-/media/files/electricity/nem/market_notices_and_events/market_event_reports/2022/nem-market-suspension-and-operational-challenges-in-june-2022.pdf (accessed 2025-02-18).

(43) Wohland, J.; Eddine Omrani, N.; Keenlyside, N.; Witthaut, D. Significant Multidecadal Variability in German Wind Energy Generation. *Wind Energy Science* **2019**, *4* (3), 515–526. https://doi.org/10.5194/wes-4-515-2019.

(44) Simshauser, P.; Gilmore, J. *Solving for "y": Demand Shocks from Australia's Gas Turbine Fleet*; Working Paper Series; Working Paper Series 2024-03; Centre for Applied Energy Economics & Policy Research, 2024; p 28.

(45) Nakamura, H.; Kobayashi, S.; Wanzala, M. A.; Adloff, F.; Cheng, L.; Cobb, A.; Dee, D.; El Akkraoui, A.; Fujiwara, M.; Hersbach, H.; Naoe, H.; Rani, S. I.; Rayner, N.; Simmons, A.; Slivinski, L.; Tanaka, T.; Thorne, P.; Yang, C.; Yin, Y.; Ayinde, A. S.; Banerjee, A.; Bosilovich, M. G.; Buela, L. C. M.; Dong, B.; Fukui, S.; Hirose, N.; Ikeuchi, H.; Krakauer, N.; Lenouo, A.; Niraula, B.; Oikonomou, C. L. G.; Sekizawa, S.; Sharma, N.; Yamazaki, A.; Yoshida, T. Toward Future Reanalyses That Meet Evolving Needs in Science, Public Services, Policymaking, and Socioeconomic Activity. *Bulletin of the American Meteorological Society* **2025**, *106* (7), E1445–E1453. https://doi.org/10.1175/BAMS-D-25-0126.1.

(46) Millstein, D.; Bolinger, M.; Wiser, R. What Can Surface Wind Observations Tell Us about Interannual Variation in Wind Energy Output? *Wind Energy* **2022**, *25* (6), 1142–1150. https://doi.org/10.1002/we.2717.

(47) Davidson, M. R.; Millstein, D. Limitations of Reanalysis Data for Wind Power Applications. *Wind Energy* **2022**, *25* (9), 1646–1653. https://doi.org/10.1002/we.2759.

(48) AEMO. *2024 Electricity Statement of Opportunities*; Australian Energy Market Operator (AEMO), 2024. https://aemo.com.au/energy-systems/electricity/national-electricity-market-nem/nem-forecasting-and-planning/forecasting-and-reliability/nem-electricity-statement-of-opportunities-esoo (accessed 2025-02-18).

(49) EY. *The Queensland Energy and Jobs Plan - Electricity Market and Economic Modelling Outcomes*; Ernst & Young (EY), Dept of Energy and Public Works - Queensland Government (QG): Brisbane, 2022. https://www.epw.qld.gov.au/energyandjobsplan/about.

(50) Energy Quest. *Energy Quarterly September 2024 - Peak Angst*; 2024.

(51) AEMO. *2025 Victorian Gas Planning Report*; Australian Energy Market Operator (AEMO), 2025. https://www.aemo.com.au/energy-systems/gas/gas-forecasting-and-planning/victorian-gas-planning-report.

(52) Lee, D. *A tale of two mega-projects: Project Energy Connect and Snowy 2.0 timelines (Part 1)*. WattClarity. https://wattclarity.com.au/articles/2024/07/a-tale-of-two-mega-projects-project-energy-connect-and-snowy-2-0-timelines-part-1/ (accessed 2025-10-05).

(53) Lee, D. *A tale of two mega-projects: Project Energy Connect and Snowy 2.0 timelines (Part 2)*. WattClarity. https://wattclarity.com.au/articles/2024/07/a-tale-of-two-mega-projects-project-energy-connect-and-snowy-2-0-timelines-part-2/ (accessed 2025-10-05).

(54) AEMO. *Gas Demand Forecasting Methodology Information Paper*; Australian Energy Market Operator (AEMO), 2025. https://aemo.com.au/energy-systems/gas/gas-forecasting-and-planning/gas-statement-of-opportunities-gsoo.

(55) Jeffrey, S. J.; Carter, J. O.; Moodie, K. B.; Beswick, A. R. Using Spatial Interpolation to Construct a Comprehensive Archive of Australian Climate Data. *Environmental Modelling & Software* **2001**, *16* (4), 309–330. https://doi.org/10.1016/S1364-8152(01)00008-1.

(56) Chua, Z.-W.; Evans, A.; Kuleshov, Y.; Watkins, A.; Choy, S.; Sun, C. Enhancing the Australian Gridded Climate Dataset Rainfall Analysis Using Satellite Data. *Scientific Reports* **2022**, *12* (1). https://doi.org/10.1038/s41598-022-25255-6.

(57) Evans, A.; Jones, D.; Smalley, R.; Lellyett, S. *An enhanced gridded rainfall analysis scheme for Australia*.

(58) Zhang, H.; Jeffrey, S.; Carter, J. Improved Quality Gridded Surface Wind Speed Datasets for Australia. *Meteorology and Atmospheric Physics* **2022**, *134* (5). https://doi.org/10.1007/s00703-022-00925-2.

(59) BoM. Himawari-8/9 Surface Global Solar Irradiance, 2025. https://www.bom.gov.au/climate/how/IDCJAD0111.shtml.

(60) BoM. Australian Hourly Solar Irradiance Gridded Data, 2022. https://www.bom.gov.au/climate/how/IDCJAD0111.shtml.

Appendix A Additional information on methodology

A.1 REZ exclusions

The N12 REZ (onshore in the Illawarra region) was excluded, as the Draft ISP-2024 did not provide CF traces for that location, and AEMO modelling projected no VRE development in that region.

For the N10 (Hunter) offshore wind REZ, CF data was produced for the floating-platform category (*FL*) but not for the fixed-platform category (*FX*), as the methodology used in this study did not identify any appropriate locations within AEMO's designated boundary. While AEMO does provide CF traces for fixed-platform windfarms in that REZ, they also designate that N10 has zero resource potential for that category.

A.2 Alternate weather datasources

Weather station data

Weather station data from the Australian Bureau of Meteorology (BoM) provides the most accurate representation of weather conditions at specific locations, however doesn't provide the necessary blend of spatial diversity, sub-daily resolution, and/or long-term temporal coverage across all the variables required for this study. BoM's automatic weather station (AWS) data has excellent temporal resolution, but insufficient longevity nor spatial coverage. Including BoM's 'synoptic' stations improves the spatial coverage, but doesn't provide hourly resolution data.

For solar modelling, the coverage of BoM's observed irradiance data is very patchy. For wind, BoM's weather station data is measured at 10m above ground level, and there was not (at the time of this study) any publicly available wind speed data measured in the range (typically 70-150m) relevant to modern turbine hub heights. There are analytical risks in using 10m wind-speed observations as a proxy for hub-height wind patterns, given (a) the relationship between the two can vary strongly over time and location; (b) evidence from other jurisdictions that 10m wind speed observations can be a poor proxy for inter-annual trends in wind turbine resource potential[46].

Interpolated grid data

To compensate for the spatio-temporal patchiness of weather station coverage, BoM and other Australian agencies have produced multiple high quality gridded datasets based on statistical interpolation across the network of observation stations. These provide a spatial resolution and temporal longevity comparable or better than the available reanalysis products; and are generally considered to be the highest quality source of Australian gridded weather data that is available.

Unfortunately, the scope of available data is insufficient for use in this study. Temperature and rainfall datasets only provide timeseries at daily resolution – insufficient for use in VRE resource modelling.[55–57] A previously documented gridded dataset for windspeed has not been publicly released, and only covers ground-level wind estimates.[58] BoM also provides satellite-derived gridded datasets for solar irradiance, but they only go back as far as the year 1990.[59,60]

A.3 Reanalysis variables used in this study

Table A1: Reanalysis variables used for the power modelling

BARRA-R2 *(wind modelling)*	Variable name	Measurement			Modifications
		units	type^	reported%	
windspeed - 100m	ua100m, va100m	m/s	instant	hour	vector magnitude
windspeed - 150m	ua150m, va150m	m/s	instant	hour	vector magnitude
roughness length	z0	m	average	daily	--
surface pressure	ps	Pa	instant	hour	--
surface temperature	tas	K	instant	hour	--

ERA5 *(wind modelling)*	Variable name	Measurement			Modifications
		units	type^	reported%	
windspeed - 100m	100u, 100v	m/s	instant	hour	vector magnitude
roughness length	fsr	m	instant	hour	--
surface pressure	sp	Pa	instant	hour	--
surface temperature	2t	K	instant	hour	--

BARRA-R2 *(solar PV modelling)*	Variable name	Measurement			Modifications
		units	type^	reported%	
GHI	rsds	W/m^2	average	half-hour	--
DNI#	rsdsdir	W/m^2	average	half-hour	--
cloud cover#	clt	fraction	average	half-hour	--
surface windspeed (10m)	uas, vas	m/s	instant	hour	vector magnitude
surface temperature (2m)	tas	K	instant	hour	--

ERA5 *(solar PV modelling)*	Variable name	Measurement			Modifications
		units	type^	reported%	
GHI	ssrd	J/m^2	total	hour	converted to W/m2
DNI#	fdir	J/m^2	total	hour	converted to W/m2
cloud cover#	tcc	fraction	instant	hour	--
surface windspeed (10m)	10u, 10v	m/s	instant	hour	vector magnitude
surface temperature (2m)	2t	K	instant	hour	--

^ *instant = instantaneous measurement; average = hourly average; total = hourly sum*

% *hour = reported on the hour (i.e. at hh:00); half-hour = reported on the half-hour (i.e. at hh:30)*

DNI and cloud cover estimates were considered, but not used directly in the final methodology

A.4 REZ specific modelling inputs

Wind

For each onshore REZ that already hosts existing wind farms, a REZ-specific combination of turbine class and hub-height was chosen that provided a blend of (a) consistency with specifications for actual (existing) windfarms within that REZ; and (b) superior statistical performance in the comparisons with AEMO CF traces.

For regions without existing wind farms, no information was found indicating that AEMO's methodology varied across REZ. Hence, for each of the following three groupings, consistent assumptions were used where possible - exceptions were made when the default assumptions were clearly the worst-performing for any specific REZ:

- For onshore REZ with no existing wind farms, the combination of Class III type turbine at 150m hub-height, gave the best (or near-best) statistical fit to the AEMO CF traces in most REZ, for both the *WH* and *WM* categories. For four REZ (Q7, S7, S9, V5) those defaults were clearly the worst-performing combination, hence different choices were used for both *WH* and *WM* categories.
- For offshore locations in the *Fixed-Platform* category, Class II turbines were assumed for all REZ, as this provided the best statistical fit in most cases. 150m hub height provided the best statistical fit for four REZ, with 125m chosen for the other two.
- For offshore locations in the *Floating-Platform* category, Class I turbines clearly provided the best fit for five REZ, with the 125m hub-height assumption chosen on the basis that it minimised the calculated bias. For the two offshore zones where Class I provided clearly the worst statistical fit, Class II and 125h hub-height was assumed.

Table A2: Offshore wind turbines - Key assumptions and error correction parameters used for the modelling. Parameters shown separately for each offshore REZ in NSW (N10-N11), Victoria (V7-V8), South Australia (S10) and Tasmania (T4-T5).

REZ	Key Assumptions				Error correction parameters *(Fixed Platforms)*				Error correction parameters *(Floating Platforms)*			
	Hub-height (m)		Turbine Class		ERA5		BARRA-R2		ERA5		BARRA-R2	
	WH	*WM*	*WH*	*WM*	*α*	*β*	*α*	*β*	*α*	*β*	*α*	*β*
N10		125		2	--	--	--	--	1.18	-1.46	1.05	-0.86
N11	150	125	2	2	2.29	-5.17	1.62	-3.16	1.53	-2.66	1.50	-3.38
V7	150	125	2	1	1.15	-0.84	1.07	-0.84	1.05	-0.48	1.02	-0.60
V8	125	125	2	1	1.45	-3.27	1.34	-3.06	1.28	-2.24	1.23	-1.98
S10	125	125	2	1	1.43	-3.17	1.36	-3.38	2.40	-9.24	1.21	-2.00
T4	150	125	2	1	1.28	-1.84	1.10	-0.99	1.39	-3.13	1.28	-2.82
T5	150	125	2	1	1.05	-0.15	0.97	-0.23	1.26	-2.14	1.16	-1.79

Table A3: Onshore wind turbines - Key assumptions and error correction parameters used for the modelling.

Parameters shown separately for each onshore REZ in Qld (Q1-Q9), NSW (N1-N9), Victoria (V1-V6), South Australia (S1-S9) and Tasmania (T1-T3).

REZ	Key Assumptions				Error correction parameters *(Wind-High)*				Error correction parameters *(Wind-Medium)*			
	Hub-height (m)		Turbine Class		ERA5		BARRA-R2		ERA5		BARRA-R2	
	WH	*WM*	*WH*	*WM*	*α*	*β*	*α*	*β*	*α*	*β*	*α*	*β*
Q1	125	150	3	3	0.89	0.97	0.81	0.97	1.00	0.55	0.83	0.55
Q2	150	150	3	3	1.56	-2.42	1.56	-2.42	1.25	-1.01	1.25	-1.01
Q3	150	150	3	3	1.94	-3.11	1.94	-3.11	1.62	-1.35	1.62	-1.35
Q4	150	150	3	3	1.49	-2.32	1.49	-2.32	1.36	-1.33	1.36	-1.33
Q5	150	150	3	3	1.25	-1.69	1.25	-1.69	1.27	-2.00	1.27	-2.00
Q6	150	150	3	3	1.69	-2.51	1.69	-2.51	1.42	-1.17	1.42	-1.17
Q7	100	150	2	3	1.67	-2.34	1.67	-2.34	1.44	-1.48	1.44	-1.48
Q8	150	150	3	3	1.51	-2.12	1.51	-2.12	1.50	-2.39	1.50	-2.39
Q9	150	150	3	3	1.52	-2.21	1.52	-2.21	1.50	-2.27	1.50	-2.27
N1	150	150	3	3	1.12	-0.44	1.12	-0.44	1.49	-3.08	1.49	-3.08
N2	150	150	3	3	1.53	-1.59	1.53	-1.59	1.51	-1.33	1.51	-1.33
N3	150	150	3	3	1.34	-1.43	1.34	-1.43	1.39	-1.74	1.39	-1.74
N4	100	100	2	2	1.24	-1.83	1.24	-1.83	1.27	-2.19	1.27	-2.19
N5	150	150	3	3	1.36	-2.95	1.36	-2.95	1.20	-1.75	1.20	-1.75
N6	150	150	3	3	1.32	-2.47	1.32	-2.47	1.10	-1.00	1.10	-1.00
N7	150	150	3	3	2.20	-4.42	2.20	-4.42	1.54	-1.00	1.54	-1.00
N8	150	150	3	3	1.85	-1.07	1.85	-1.07	1.35	0.54	1.35	0.54
N9	150	150	3	3	1.33	-0.21	1.33	-0.21	1.44	-0.92	1.44	-0.92
V1	150	150	3	3	1.51	-0.18	1.51	-0.18	2.13	-3.15	2.13	-3.15
V2	150	150	3	3	1.10	-1.29	1.10	-1.29	1.22	-2.10	1.22	-2.10
V3	150	150	3	3	1.30	-1.64	1.30	-1.64	1.23	-1.62	1.23	-1.62
V4	100	150	1	3	0.92	0.06	0.92	0.06	1.16	-1.72	1.16	-1.72
V5	100	100	2	2	0.99	0.08	0.99	0.08	0.96	-0.11	0.96	-0.11
V6	150	150	3	3	1.34	-2.09	1.34	-2.09	1.24	-1.57	1.24	-1.57
S1	100	125	1	2	1.18	-1.15	1.18	-1.15	1.29	-1.67	1.29	-1.67
S2	150	150	3	3	1.16	-1.63	1.16	-1.63	1.17	-1.51	1.17	-1.51
S3	150	150	3	3	1.18	-0.77	1.18	-0.77	1.49	-2.82	1.49	-2.82
S4	100	100	1	2	1.13	-0.68	1.13	-0.68	1.12	-0.82	1.12	-0.82
S5	150	150	3	3	1.40	-2.42	1.40	-2.42	1.30	-1.58	1.30	-1.58
S6	150	150	3	3	1.31	-1.45	1.31	-1.45	1.35	-1.99	1.35	-1.99
S7	125	125	2	2	1.08	-0.94	1.08	-0.94	1.10	-1.03	1.10	-1.03
S8	125	150	2	3	1.37	-1.72	1.37	-1.72	1.17	-0.97	1.17	-0.97
S9	125	125	2	2	1.17	-1.03	1.17	-1.03	1.22	-0.87	1.22	-0.87
T1	100	100	1	1	1.31	-2.59	1.31	-2.59	1.06	-0.83	1.06	-0.83
T2	125	125	2	2	1.30	-1.89	1.30	-1.89	1.25	-1.62	1.25	-1.62
T3	150	150	3	3	1.44	0.06	1.44	0.06	1.41	0.37	1.41	0.37

Solar PV

Figure A1: Profile of weekly correction factors used in the solar PV error correction process.

Factors plotted separately for each onshore REZ in Qld (Q1-Q9), NSW (N1-N9), Victoria (V1-V6), South Australia (S1-S9) and Tasmania (T1-T3).

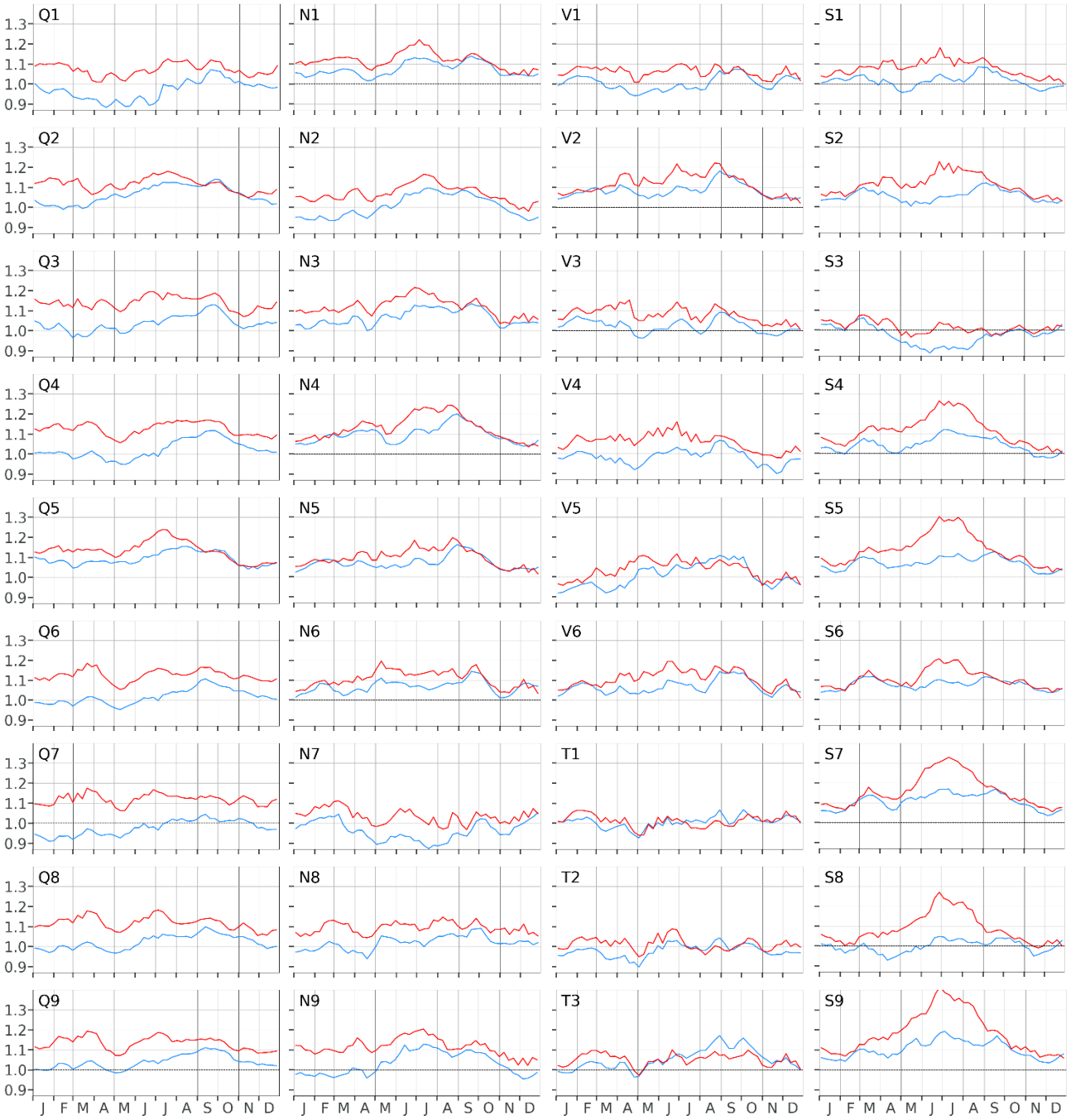

Appendix B Additional results

Table B1: Statistical comparison (model vs AEMO) of the CF results, for the 2010-11 to 2022-23 period.

Equivalent analyses are shown for the CF results (a) before and (b) after the error correction steps are applied.

For each metric, the 10th percentile and 90th percentile (p10/p90) of the REZ-specific results is shown – for wind, these metrics are calculated across all onshore (WH, WM) and offshore (FX, FL) categories.

Bias is the difference [model – AEMO] of CF means. For the variance indicators (Std Dev; p10-p90 range), ratios are calculated as [model / AEMO]. Pearson correlation coefficient and root-mean-square error (RMSE) are shown for comparisons of the modelled hourly CF, also for daily- and weekly-averaged CF.

(a)		Bias	ratio of…		correlation			RMSE		
			Std Dev.	p10-p90	hourly	daily	weekly	hourly	daily	weekly
Wind	ERA5	-0.159 / 0.029	0.69 / 0.97	0.64 / 0.96	0.80 / 0.93	0.85 / 0.94	0.87 / 0.95	0.11 / 0.23	0.08 / 0.20	0.04 / 0.18
	BARRA-R2	-0.088 / 0.089	0.86 / 1.03	0.84 / 1.04	0.76 / 0.89	0.85 / 0.93	0.88 / 0.95	0.13 / 0.21	0.09 / 0.15	0.05 / 0.11
Solar	ERA5	-0.021 / 0.005	0.83 / 0.92	0.81 / 0.91	--	0.86 / 0.93	0.94 / 0.98	--	0.05 / 0.06	0.02 / 0.03
	BARRA-R2	-0.008 / 0.017	0.75 / 0.89	0.69 / 0.88	--	0.86 / 0.93	0.92 / 0.98	--	0.05 / 0.06	0.02 / 0.03

(b)		Bias	ratio of…		correlation			RMSE		
			Std Dev.	p10-p90	hourly	daily	weekly	hourly	daily	weekly
Wind	ERA5	-0.001 / 0.001	0.99 / 1.00	0.96 / 1.00	0.79 / 0.93	0.84 / 0.95	0.86 / 0.95	0.10 / 0.19	0.07 / 0.13	0.03 / 0.07
	BARRA-R2	-0.001 / 0.001	0.99 / 1.00	0.96 / 1.00	0.76 / 0.89	0.85 / 0.93	0.88 / 0.95	0.13 / 0.21	0.08 / 0.14	0.04 / 0.07
Solar	ERA5	-0.001 / 0.001	0.84 / 0.92	0.81 / 0.90	--	0.86 / 0.93	0.94 / 0.98	--	0.04 / 0.06	0.02 / 0.03
	BARRA-R2	0.000 / 0.002	0.76 / 0.88	0.71 / 0.87	--	0.86 / 0.93	0.93 / 0.98	--	0.05 / 0.06	0.02 / 0.03

Wind CF comparison (modelled-CF vs AEMO-CF)

Figure B1: Comparison of modelled wind CF vs the AEMO-CF benchmark.

Results are shown for the modelled CF using ERA5 (left panels) and BARRA-R2 (right panels); then repeated for the hourly modelled CF, daily-avg CF and weekly-avg CF. Within each panel, the results are separated by the 4-monthly seasonal grouping (summer; bridge; winter).

Hourly

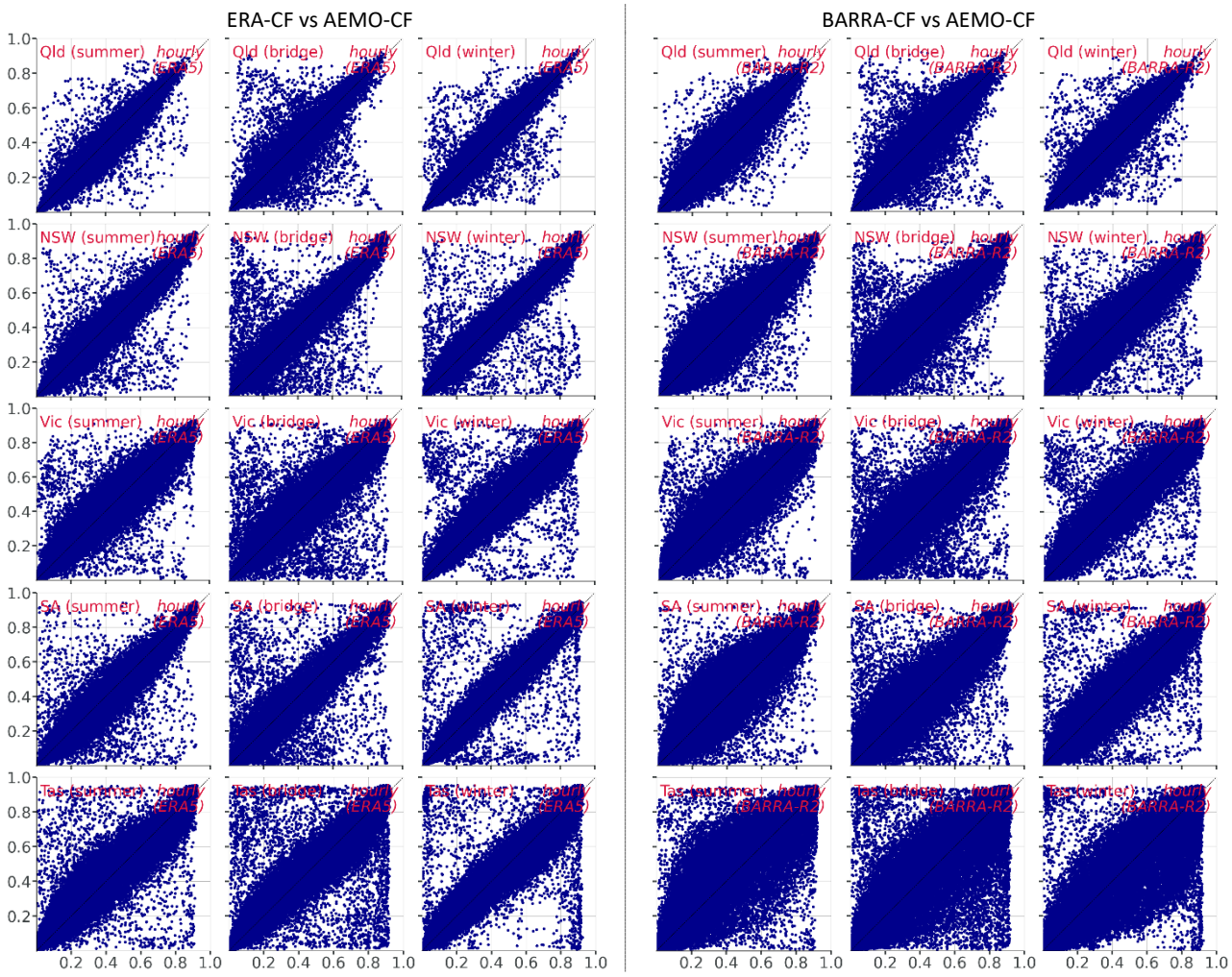

Daily

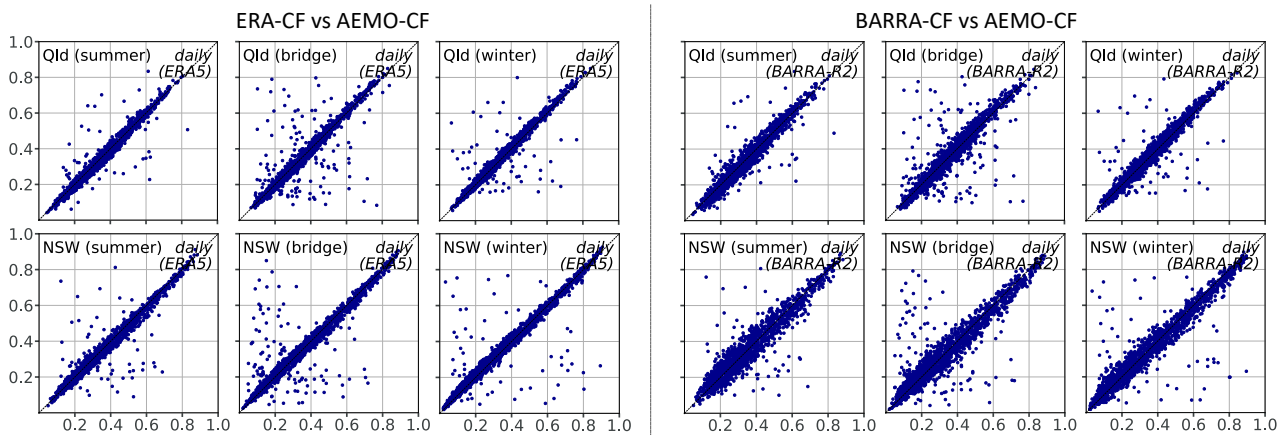

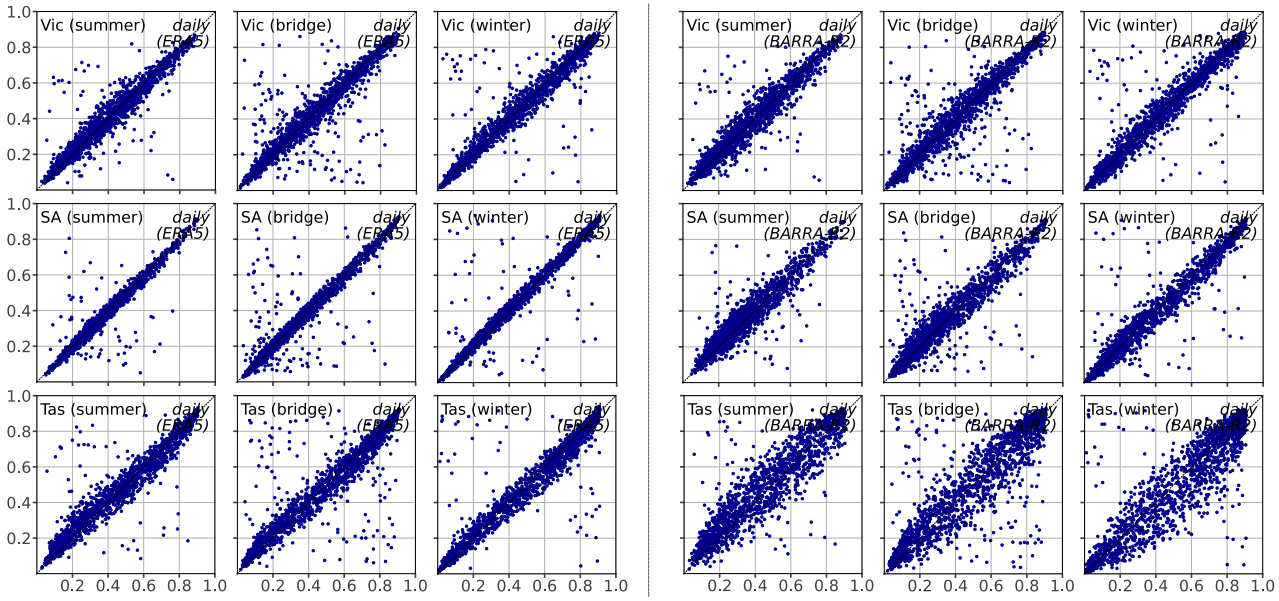
Vic (summer) daily (ERA5)
Vic (bridge) daily (ERA5)
Vic (winter) daily (ERA5)
SA (summer) daily (ERA5)
SA (bridge) daily (ERA5)
SA (winter) daily (ERA5)
Tas (summer) daily (ERA5)
Tas (bridge) daily (ERA5)
Tas (winter) daily (ERA5)
Vic (summer) daily (BARRA-R2)
Vic (bridge) daily (BARRA-R2)
Vic (winter) daily (BARRA-R2)
SA (summer) daily (BARRA-R2)
SA (bridge) daily (BARRA-R2)
SA (winter) daily (BARRA-R2)
Tas (summer) daily (BARRA-R2)
Tas (bridge) daily (BARRA-R2)
Tas (winter) daily (BARRA-R2)

Weekly

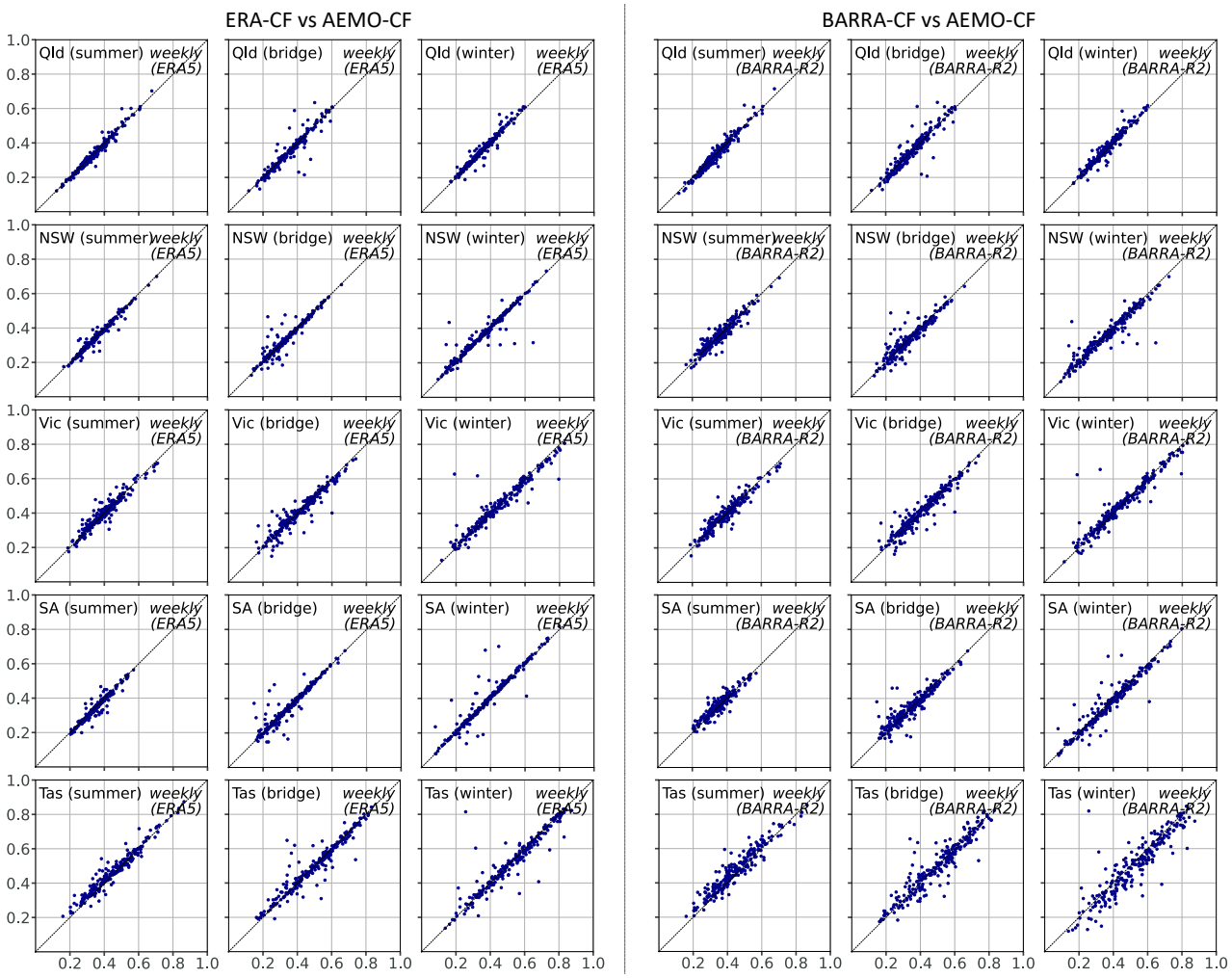
ERA-CF vs AEMO-CF
BARRA-CF vs AEMO-CF
Qld (summer) weekly (ERA5)
Qld (bridge) weekly (ERA5)
Qld (winter) weekly (ERA5)
NSW (summer) weekly (ERA5)
NSW (bridge) weekly (ERA5)
NSW (winter) weekly (ERA5)
Vic (summer) weekly (ERA5)
Vic (bridge) weekly (ERA5)
Vic (winter) weekly (ERA5)
SA (summer) weekly (ERA5)
SA (bridge) weekly (ERA5)
SA (winter) weekly (ERA5)
Tas (summer) weekly (ERA5)
Tas (bridge) weekly (ERA5)
Tas (winter) weekly (ERA5)
Qld (summer) weekly (BARRA-R2)
Qld (bridge) weekly (BARRA-R2)
Qld (winter) weekly (BARRA-R2)
NSW (summer) weekly (BARRA-R2)
NSW (bridge) weekly (BARRA-R2)
NSW (winter) weekly (BARRA-R2)
Vic (summer) weekly (BARRA-R2)
Vic (bridge) weekly (BARRA-R2)
Vic (winter) weekly (BARRA-R2)
SA (summer) weekly (BARRA-R2)
SA (bridge) weekly (BARRA-R2)
SA (winter) weekly (BARRA-R2)
Tas (summer) weekly (BARRA-R2)
Tas (bridge) weekly (BARRA-R2)
Tas (winter) weekly (BARRA-R2)

Solar CF comparison (modelled-CF vs AEMO-CF)

Figure B2: Comparison of modelled solar CF (hourly, daily- & weekly-avg) vs the AEMO-CF benchmark.

Results are shown for the modelled CF using ERA5 (left panels) and BARRA-R2 (right panels); then repeated for the daily-avg CF and weekly-avg CF. Each panel separates results by seasonal grouping (summer; bridge; winter).

Daily

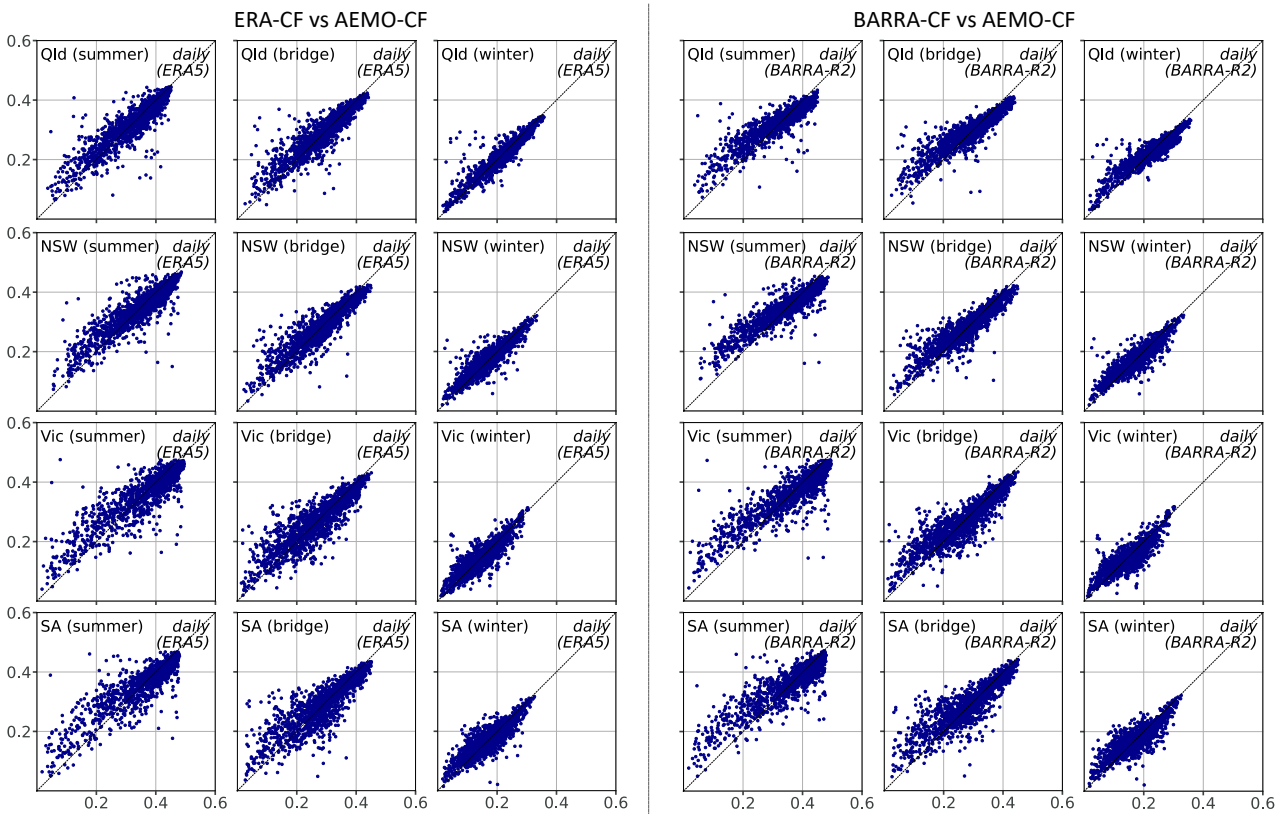

Weekly

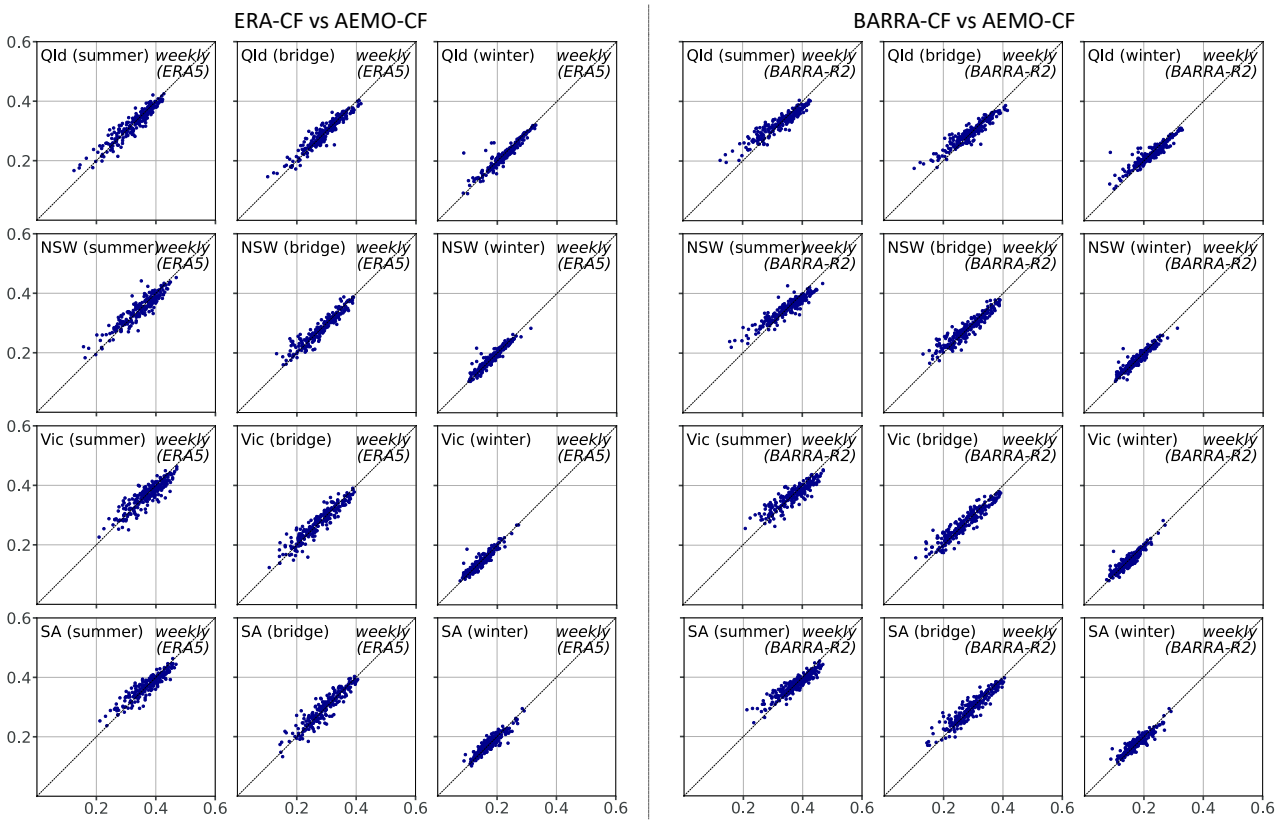

CF distributions

The following plots illustrate the CF distributions using a 'generation-duration' curve – the x-axis shows the % of hours for which the CF is below the value shown on the y-axis.

Figure B3: Generation-duration curves for daily wind- and solar-CF (2011-2023), comparing UQ results with AEMO. Within each panel (Wind; Solar), results are separated by the 4-monthly seasonal grouping (summer; bridge; winter).

Wind

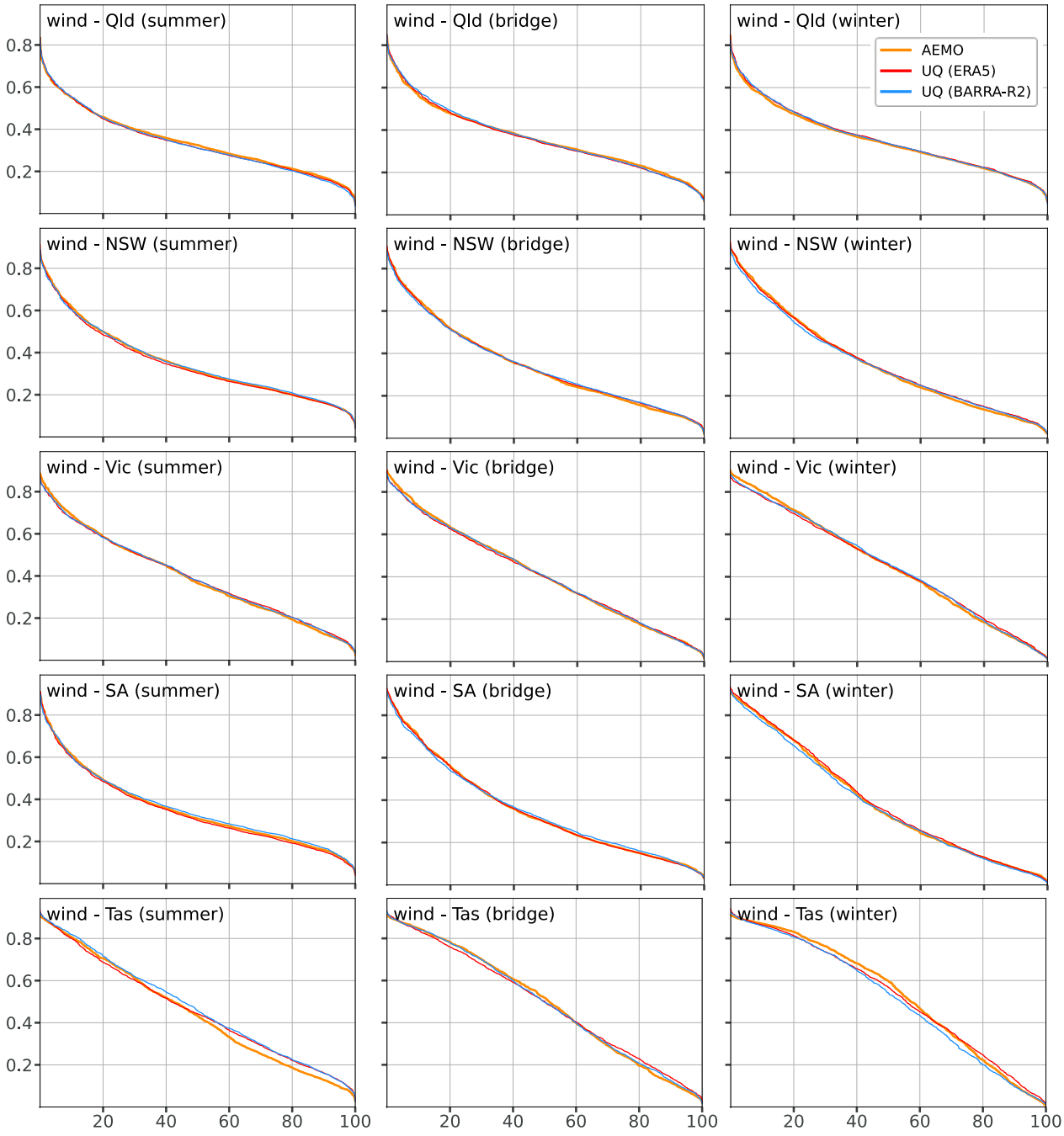

Solar

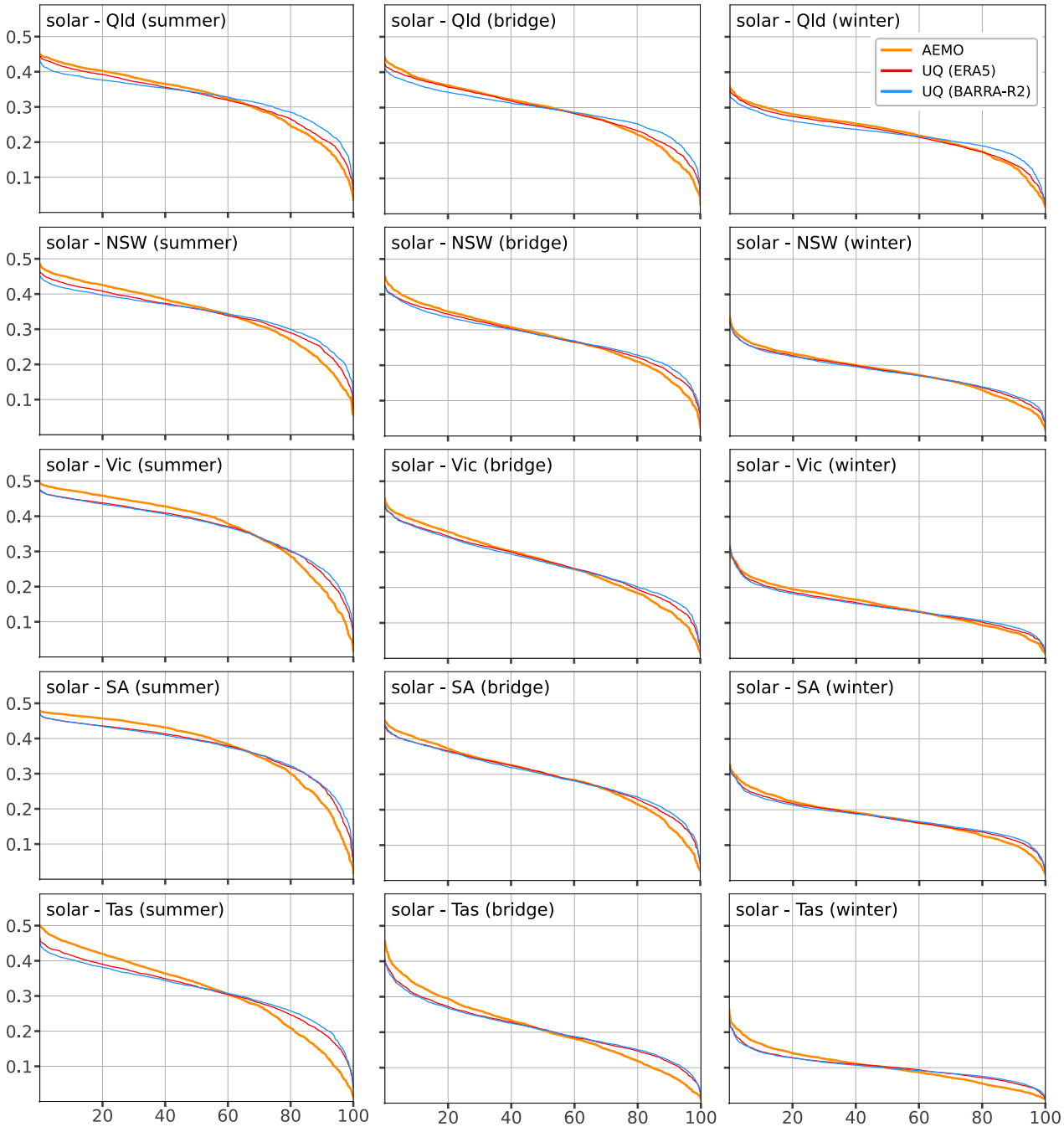
solar - Qld (summer)
solar - Qld (bridge)
solar - Qld (winter)
AEMO
UQ (ERA5)
UQ (BARRA-R2)
solar - NSW (summer)
solar - NSW (bridge)
solar - NSW (winter)
solar - Vic (summer)
solar - Vic (bridge)
solar - Vic (winter)
solar - SA (summer)
solar - SA (bridge)
solar - SA (winter)
solar - Tas (summer)
solar - Tas (bridge)
solar - Tas (winter)
0.5
0.4
0.3
0.2
0.1
20
40
60
80
100

Seasonal fit

The following plots provide the seasonal profile of 30d-avg CF, shown as a spread (minimum to maximum) across the 2011-2023 period. Both the ERA and BARRA models are compared to the ISP values. State-level plots are based on a capacity-weighted average of the smoothed (rolling 30d-avg) CF time-series for each REZ. Results are shown for the uncorrected (raw) and corrected CF results.

Figure B4: Seasonal spread of the wind- and solar-CF across 2011-2022, comparing modelled vs AEMO results.

Tasmanian solar CF results show an unweighted average across REZ, as the ISP scenario results have zero solar capacity in those REZ. All other states (and all wind results) use the default weighted-average method for aggregation across REZ.

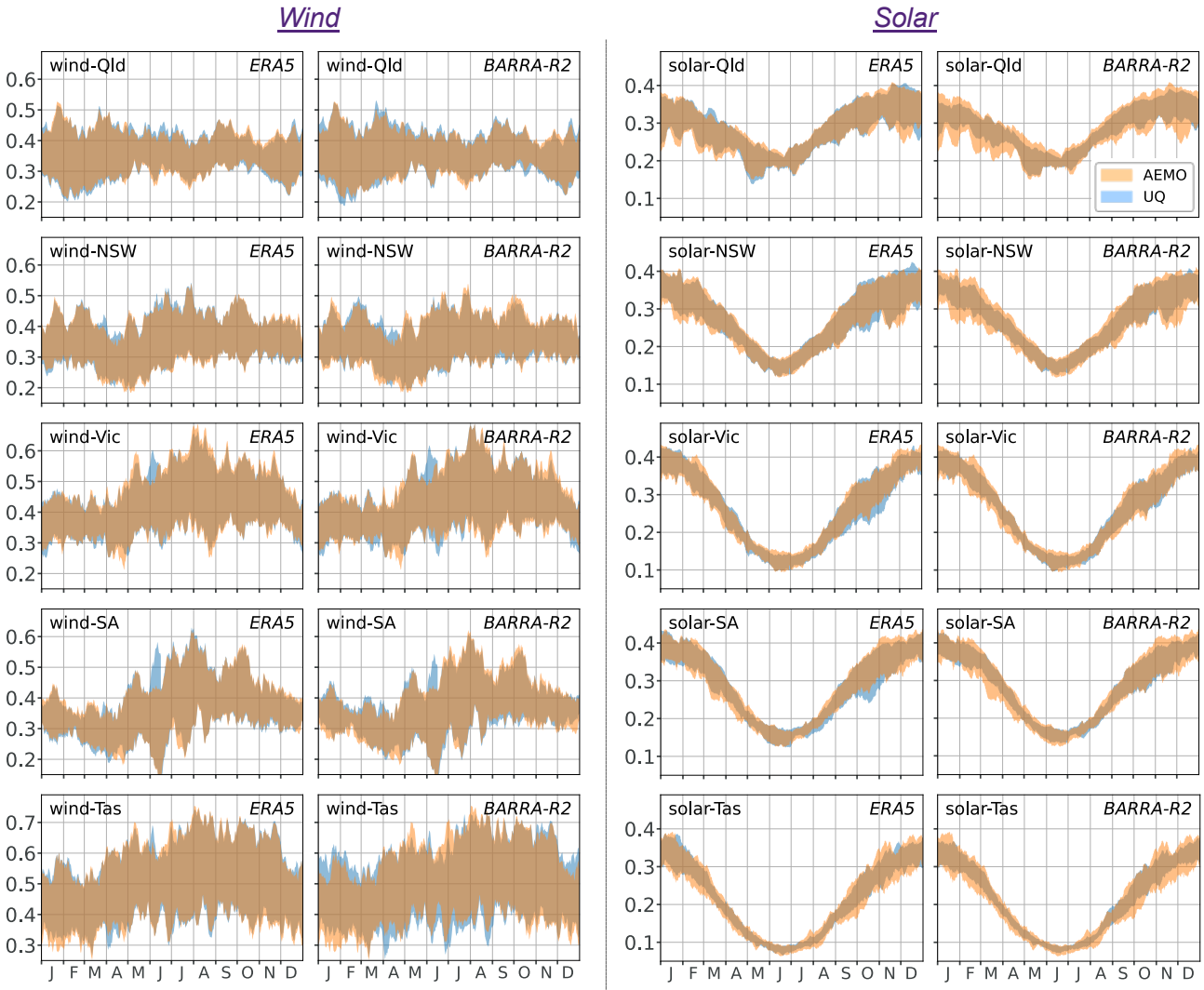

Decadal change in the spread of 30-day CF

The following plots provide the seasonal profile of 30-day averaged CF, shown as a spread (minimum to maximum) across each period shown in the legend. State-level plots are based on a capacity-weighted average of the smoothed (rolling 30d-avg) CF time-series for each REZ.

Results are shown for the CF modelled using the ERA5 reanalysis product.

Figure B5: Seasonal spread of the wind- and solar-CF modelled using ERA5, comparing across historical periods.

Wind CF

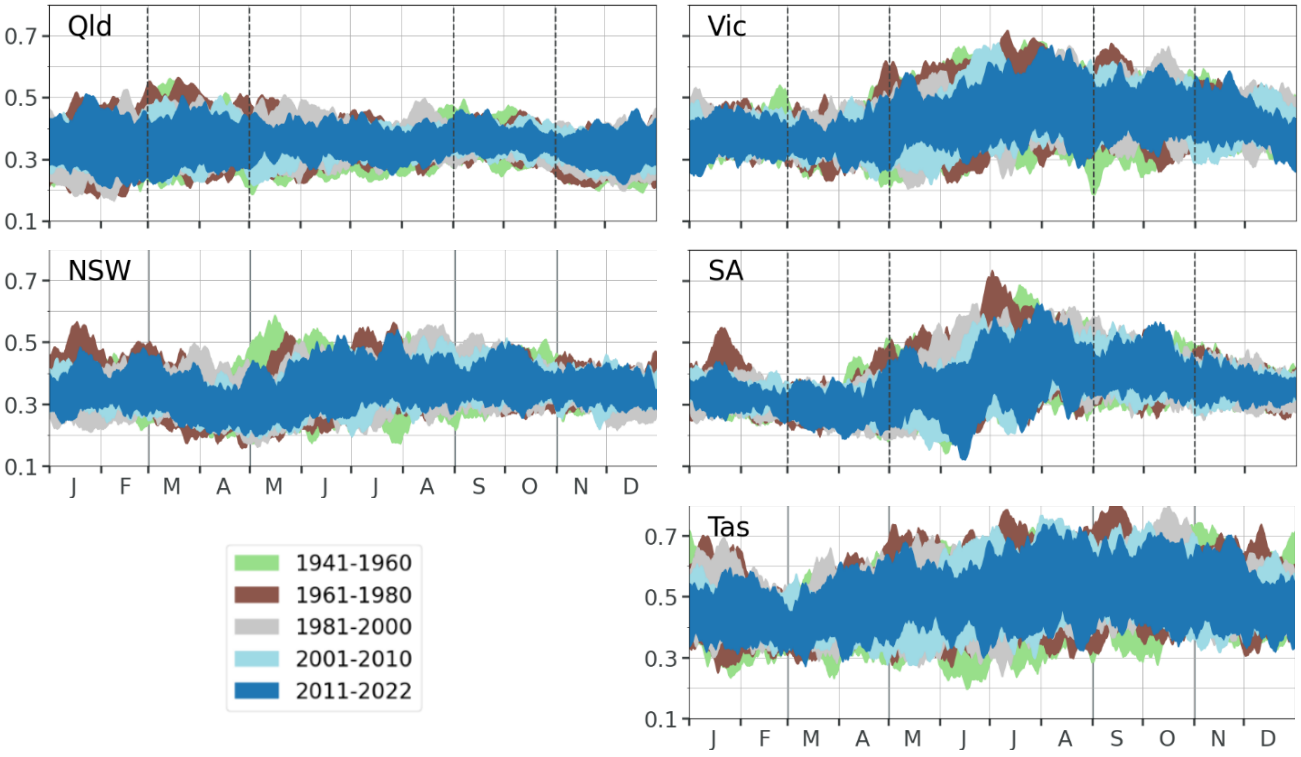

Solar CF

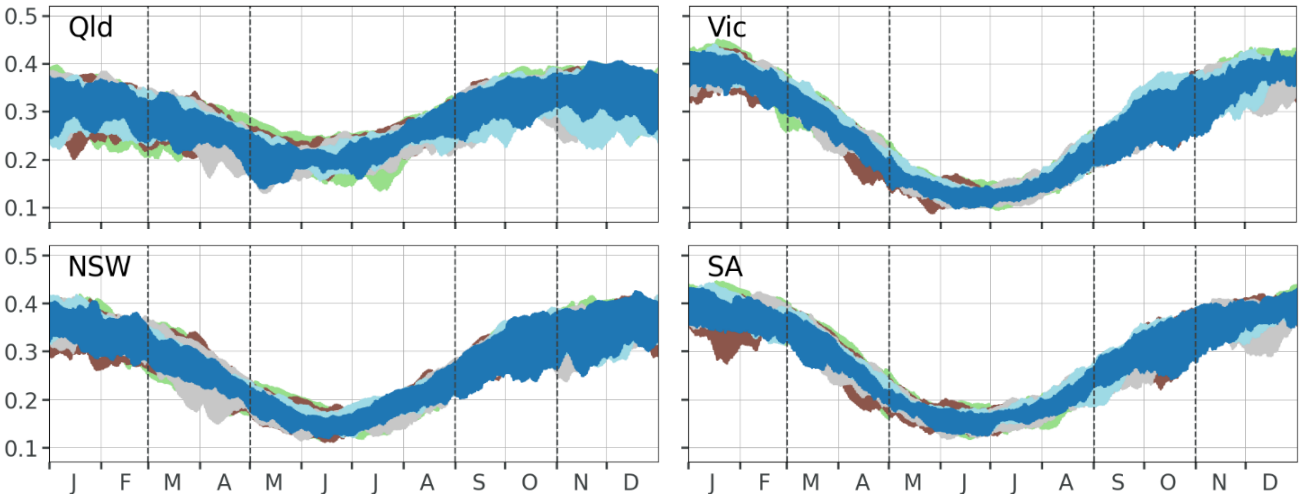

Inter-annual quantiles of weekly CF

The following plots show the long-term trend in 10th percentile (p10) and median (p50) of 7-day CF. For each year, the quantiles are calculated from the values produced by a 7-day rolling average across the CF timeseries. Bands show the spread (across 2011-2022) of equivalent 10th percentile values from the AEMO CF traces.

Figure B6: Inter-annual variation in quantiles of seasonal CF, for wind and solar.

Wind

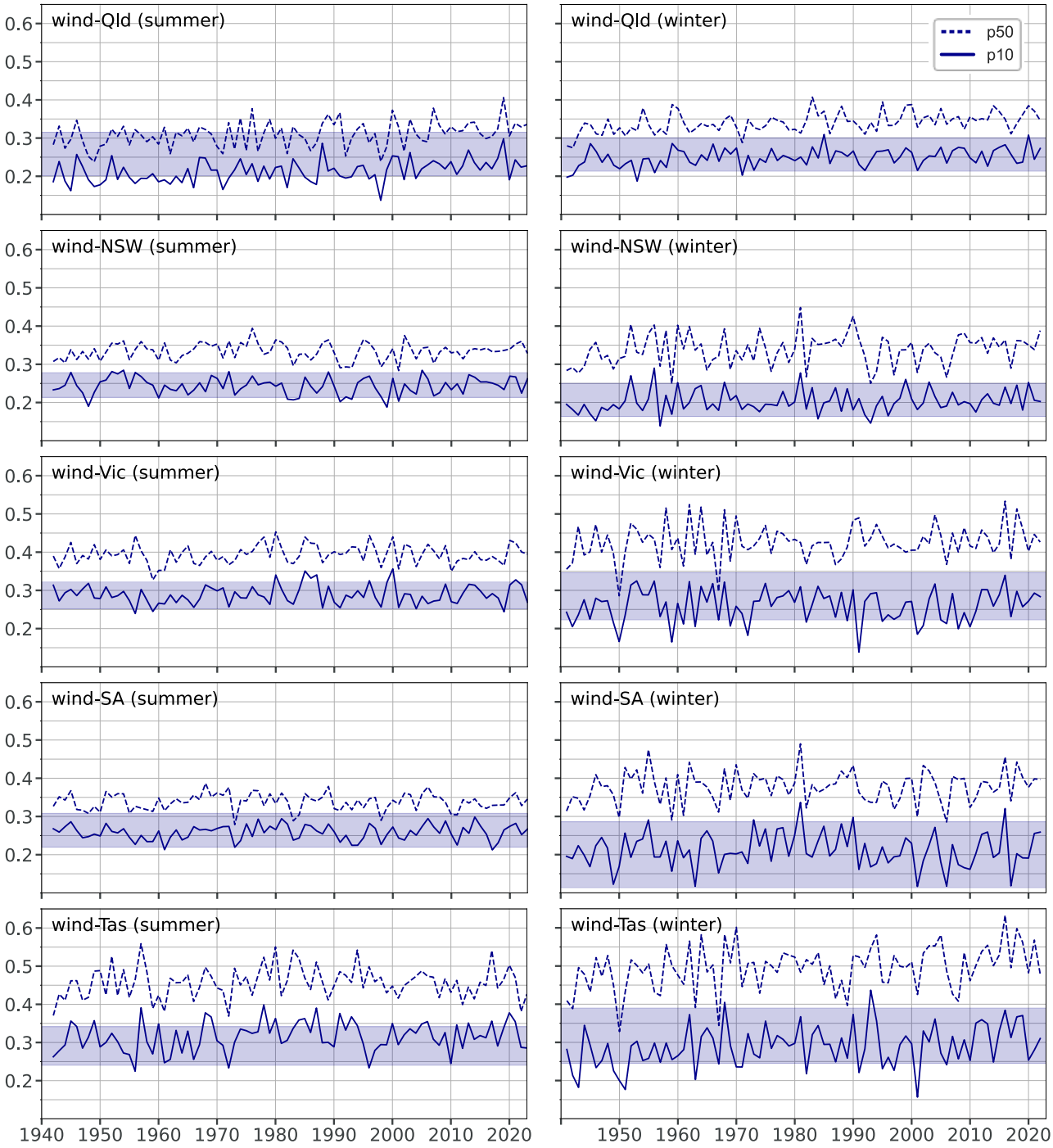

Solar

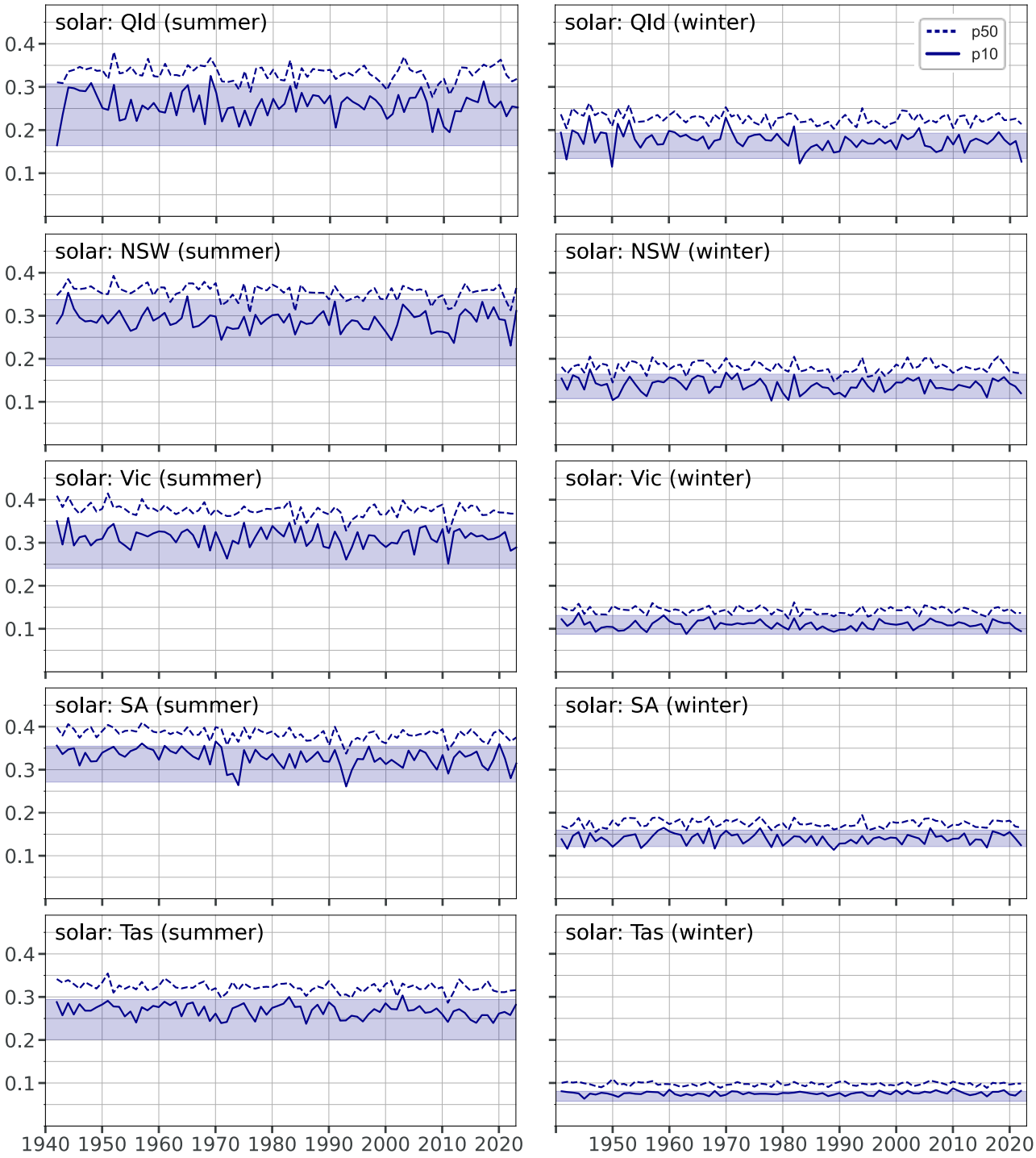
solar: Qld (summer)
solar: Qld (winter)
p50
p10
solar: NSW (summer)
solar: NSW (winter)
solar: Vic (summer)
solar: Vic (winter)
solar: SA (summer)
solar: SA (winter)
solar: Tas (summer)
solar: Tas (winter)
0.4
0.3
0.2
0.1
1940 1950 1960 1970 1980 1990 2000 2010 2020
1950 1960 1970 1980 1990 2000 2010 2020

THE UNIVERSITY OF QUEENSLAND
AUSTRALIA

CREATE CHANGE

Contact details

Dr Joe Lane
T +61 7 3346 4028
E joe.lane@uq.edu.au
W gas-energy.centre.uq.edu.au

CRICOS Provider Number 00025B